Identification of neurons controlling orientation behavior in the *Drosophila melanogaster* larva

Julia Riedl

Tesi Doctoral - 2013

Thesis Director

Dr. Matthieu Louis

Sensory Systems and Behaviour
EMBL-CRG Systems Biology Unit

UNIVERSITAT POMPEU FABRA

„Der Wert eines Dialogs hängt vor allem von der Vielfalt der konkurrierenden Meinungen ab."

Sir Karl Popper

Abstract

Detecting sensory stimuli and converting them into behavioral output is the essential function of nervous systems. When faced with a gradient of environmental cues animals can infer its direction and orient accordingly, a reaction vital for detecting food or mates and for avoiding noxious agents. In this study we took advantage of the numerical simplicity of the nervous system of the *Drosophila melanogaster* larva to find neurons underlying orientation behavior to chemical cues (chemotaxis). To this aim we performed a large behavioral screen using the Gal4/UAS system to express a synaptic silencing toxin in genetically defined subpopulations of neurons. Subsequent high-resolution analysis of behavioral impairments caused by the neural loss of function revealed neurons responsible for correct execution of taxis behavior. We identified a Gal4 line (NP4820) covering a subgroup of neurons in the suboesophageal ganglion (SOG) of the larval brain to be involved in the organization of the specific behavioral modes underlying orientation behaviors. Larvae devoid of functional NP4820-labeled neurons were impaired in the correct transition from run- to casts/turn- mode in respect to sensory experience. Strikingly, remotely activating the neurons was sufficient to initiate a cast/turn maneuver. The effect could be generalized to other sensory modalities than olfaction, suggesting the SOG as a brain region generally essential for action selection and execution.

Using the same approach we searched for neurons underlying orientation in a static electric field. Detailed analysis of electrotactic behavior showed that *Drosophila* larvae robustly migrate to the cathode, making use of cast/turn maneuvers to align to the field. Moreover, our

behavioral screen revealed electrosensory neurons located in the larval terminal organ, projecting to the SOG. Functional imaging showed that their neural activity is tuned to the orientation and amplitude of the field, underlying the ability of the larva to align with the local electric field. Our findings revealed the existence of a novel sensory modality in *Drosophila melanogaster* and support the growing evidence that electric fields represent a biologically relevant stimulus.

Resumen

La función esencial del sistema nervioso es detectar estímulos sensoriales y transformarlos en respuestas conductuales. Al detectar gradientes de señales ambientales los animales pueden deducir su dirección y orientarse en consecuencia, es una reacción vital para identificar comida o aparearse y así evitar agentes nocivos. En este estudio hemos aprovechado la simplicidad numérica del sistema nervioso de la larva de la *Drosophila melanogaster* para identificar las neuronas responsables que dirigen sus movimientos de acuerdo a ciertas sustancias químicas (quimiotaxis). Con este propósito, hemos realizado un amplio rastreo conductual utilizando el sistema Gal4/UAS para expresar en subpoblaciones de neuronas genéticamente definidas una toxina silenciadora de la sinapsis. Subsiguientes análisis de alta resolución a cerca de las deficiencias del comportamiento causadas por la pérdida de la función neuronal revelaron las neuronas responsables del comportamiento hacia gradientes químicos. Hemos identificado una línea Gal4 (NP4820) perteneciente al subgrupo de neuronas del ganglio subesofágico (GSO) del cerebro de la larva involucrada en la organización de modalidades conductuales específicas subyacentes al comportamiento orientativo. Las larvas desprovistas de neuronas marcadas-NP4820 funcionales se vieron afectadas en cuanto a la correcta transición de una trayectoria recta a un movimiento de rastreo/giro respecto a su experiencia sensorial. Notablemente, activar las neuronas remotamente fue suficiente para iniciar la maniobra de rastreo/giro. Este efecto puede generalizarse a otras modalidades sensoriales a parte del olfato, sugiriendo así el GSO como una región del cerebro esencial para seleccionar y ejecutar acciones.

Utilizando la misma estrategia buscamos neuronas responsables de la orientación en campos electrostáticos. Un análisis detallado del comportamiento electrostático ha demostrado que las larvas de *Drosophila* migran claramente hacia el cátodo, basándose en maniobras de rastreo/giro para alinearse al campo eléctrico. Además, nuestro rastreo conductual ha revelado neuronas eletrosensoriales localizadas en el órgano terminal de la larva, que proyectan en el GSO. La toma de imágenes funcionales ha demostrado que su actividad neuronal depende de la orientación y amplitud del campo, sustentando así la habilidad de la larva para alinearse al campo eléctrico local. Nuestros descubrimientos revelan la existencia de una nueva modalidad sensorial en la *Drosophila melanogaster* y respaldan la creciente evidencia que el campo eléctrico representa un estímulo biológicamente relevante.

Acknowledgements

First I want to thank Matthieu Louis and the Centre de Regulació Genomica for giving me the opportunity to pursue the endeavor of this doctoral study. Matthieu, who was willing to share his devotion and energy, all the excitement and disappointment along the way. Equally, for exposing himself to opposing viewpoints and long discussions, always being careful and uttering his honest opinion. I am very grateful for him to create an atmosphere which so much fosters independent thinking, even more as this means to cope with the challenging task of earnestly dealing with a range of very different personalities. I tremendously enjoyed being surrounded by this variety of thoughts and people for the last 5 years. I want to thank Aljoscha, Andreas, Alex, Sam, Mariana, Moraea and Ibrahim for the support, the laughter, the scientific and political discussions, for being home and work at the same time. Many thanks also to the helpful CRG community for making work efficient and exciting. I also want to thank Matthieu and our collaborators for giving me the possibility to work and learn about science in various different places. Learning and interacting with the people at Janelia Farm Research Campus was an extraordinary experience and absolutely inspiring. Equally I enjoyed very much working with the Kadow lab at MPI Munich; it was a fruitful collaboration making the project actually possible. Thanks to Ilona for including me in her team, for support and encouragement. Thanks to Verena for the great help and collaboration, equally to all the Kadow lab members for the great atmosphere and the good time.

I am deeply grateful to my parents, family and friends in Vienna, who always accompanied me, shared good and bad times with love and support, generously helping with lots of talking and sponsoring plane tickets. Thanks especially to my parents for having always encouraged curiosity and independence. Finally, I want to thank the wonderful people I met and shared time with in Barcelona. They helped me to gain new views on life, to see the irony and beauty in everything, which allows putting things- including this work- in perspective.

Preface

The staggering complexity and the elusive function of nervous systems have fascinated scientists for centuries. The pioneering histological work of Santiago Ramon y Cajal in the 1800s established that a brain consists of discrete neural cells connected in a highly complex manner. However, our understanding how these networks function remains limited. How does the delicate balance of a brains various constituents- its neurons, neurotransmitters, synapses- lead to meaningful behavioral output enabling an organism to interact with its environment? Moreover, can we ultimately seek to understand how the human brain functions, aiming to treat neurodegenerative or psychiatric diseases? In the last decades, the rise of life sciences and molecular biology also impressively advanced neurobiology research. The scientific community now possesses unprecedented means to investigate neural circuits. In this study we aimed to apply these tools to ask the fundamental question of how a neural network elicits specific behavior in response to a given stimulus. How is sensory information integrated by the brain, eventually controlling the locomotion apparatus appropriately? To this aim we studied orientation behavior in *Drosophila melanogaster* larvae: a model organism which –besides offering a tremendously large body of knowledge about its biology- has a numerically simple brain of only several 1000 neurons yet showing complex behavioral responses. The recently developed genetic techniques for *Drosophila* allowed us to manipulate the function of specific parts of its brain, identifying distinct neurons and their role in behavioral organization and execution. We found that behavioral output is controlled by a brain region which

integrates information from various sensory modalities and is involved in controlling specific behavioral output in response to the sensory inputs. Moreover, we identified a novel sensory modality: detection of electric fields, leading to orientation of the larva along the field direction. I believe that this thesis work is an example of a fruitful combination the powerful tools available for the *Drosophila* research, revealing new constituents of behavioral organization and a novel type of sensory representation.

Contents

Chapter 1:

Introduction and Aims

Nervous systems enable animals to interact with the world by integrating sensory information and transforming it into appropriate motor outputs. While sensory input and motor output are readily accessible by quantifying sensory input or the resulting behavior, the computations performed by a neural network to transform the perceived stimulus to locomotion remain mainly illusive. Understanding the organization and function of neural circuits and their cellular components is a challenging task given the extraordinary complexity of many nervous systems. Both the large number of neurons involved and their connectivity and plasticity hamper our understanding of nervous system function (Koch and Laurent 1999) . A human brain consists of staggering 90 billion neurons and even the significantly smaller mouse brain still comprises more than 70 million (Herculano-Houzel 2009). Accordingly, relatively simple invertebrate nervous systems of the size of several thousand neurons are appealing entry points to elucidate the function of this "black box". One of them, the fruit fly *Drosophila melanogaster* has proved to be a prolific model organism to understand principles of biology in general and neurobiology in particular. In fact, it was *Drosophila* research which established the field of behavioral genetics. In the 1960s, Benzer and colleagues recognized that *Drosophila* offers the same advantages to study behavior, as it did to classical genetics. Large population numbers and short generation time, as well as a rapidly growing body of knowledge about its biology, made *Drosophila* an

appealing model organism for the first studies of behavioral genetics. Benzer employed a screening approach searching for flies altered in certain behaviors such as photo- and geotaxis after mutagenesis. In this way single genes could be linked for the first time to behavior (Benzer 1967). Later, Hotta's work on sex mosaics revealed that the behavioral effects of genes could be mapped to specific regions of the nervous system. This landmark discovery connected behavior to specific neural substrates for the first time (Hotta and Benzer 1970).

Drosophila melanogaster belongs to the class of holometabola, thus going through four phases of development: embryonic, larval, pupal and adult. It has a ganglionic organization: cell bodies of neurons and glial cells build an outer layer, similar to a cortex. The axons and dendrites extend in an inner neuropil, where the highly branched extensions contact each other via synapses (Cardona, Saalfeld et al. 2009). The adult *Drosophila melanogaster* brain consists of approximately 100.000 neurons as compared to 90 billion in the human brain. Despite of its reduced size, all known human sensory modalities - and possibly even more - are represented (Figure 1.1B). Likewise, a wide gamut of behaviors can be elicited, ranging from flight and escape-responses to complex courtship "dance" or fighting between male flies (Baier, Wittek et al. 2002, Stockinger, Kvitsiani et al. 2005). At the larval stage (Figure 1.1A) the brain is even more reduced in size and number. Only an estimated 5000 neurons constitute the nervous system (Benzer 1967).This makes it an ideal model system for unraveling the building blocks of a simple nervous system, such as neural anatomy, function and connectivity. The brain consists of two anterior hemispheres (brain lobes, BL, Figure 1.1B); receiving input from sensory receptor neurons such as

thermo-, photo, chemosensory and taste neurons. In addition they are considered to be the site of sensory integration and memory formation. The posterior part is termed ventral nerve cord; it is the entry point for touch and proprioceptive as well as heat- and nociceptive neurons. It is believed to harbor the central pattern generators underlying larval crawling, as well as the interneurons essential for head movements (Berni, Pulver et al. 2012), (Fox, Soll et al. 2006) . Moreover, it is the origin of the motor-neurons conveying the behavior output to the muscles of the larva (Kohsaka, Okusawa et al. 2012).

Another crucial advantage of the fly over other invertebrates and vertebrates is its outstanding amenability to genetic manipulations. Based on the seminal work of Benzer and others, the recent surge of genetic tools gives us unprecedented possibilities to interact with the function of unambiguously defined parts of the nervous systems — a feat that was unimaginable just a decade ago. From using genetics to roughly affiliating cell substrates or body parts with altered behavior in the 1960s, we proceeded to ever more sophisticated manipulations. We are now able to interact in subtle ways with the function of single neurons: changing and controlling specific physiological properties such as spiking activity or neurotransmitter release allows us to get insight in their function. Two parallel technological developments have mainly contributed to this advance: the UAS/Gal4 binary expression system (Figure 1.1C), which allows targeting of gene products to defined sets of cells. Gal4 is a yeast transcription factor which binds and activates the UAS promotor and the genes lying under its direct downstream control. Transgenic flies expressing Gal4 under the control of a fly promotor activate the expression of “target” genes under regulation of the UAS-sequence.

Therefore, a specific Gal4 line can control expression of any wished gene in a transgenic fly in which UAS sites were inserted upstream of the specific target gene. Lately the available “payloads” for this system have been extended to a large set of tools comprising neural activators, inhibitors anatomical markers, and proteins to monitor neural activity. While the repertoire of UAS and Gal4 lines continues to expand, use of e.g. temperature sensitive variants or intersection of gene expression and suppression allows both spatial and temporal control of gene function. Moreover, parallel binary expression systems have been developed, using the same strategy but different transcriptional activator proteins and upstream sequences (Lai and Lee 2006, Potter, Tasic et al. 2010). Combination of these systems allows to differentially express various effectors and the employment of “logical gates” when targeting overlapping cell populations. Taken together, this provides us with a set of powerful tools for the quest of probing nervous systems and understanding how subsets of neurons contribute to behavior.

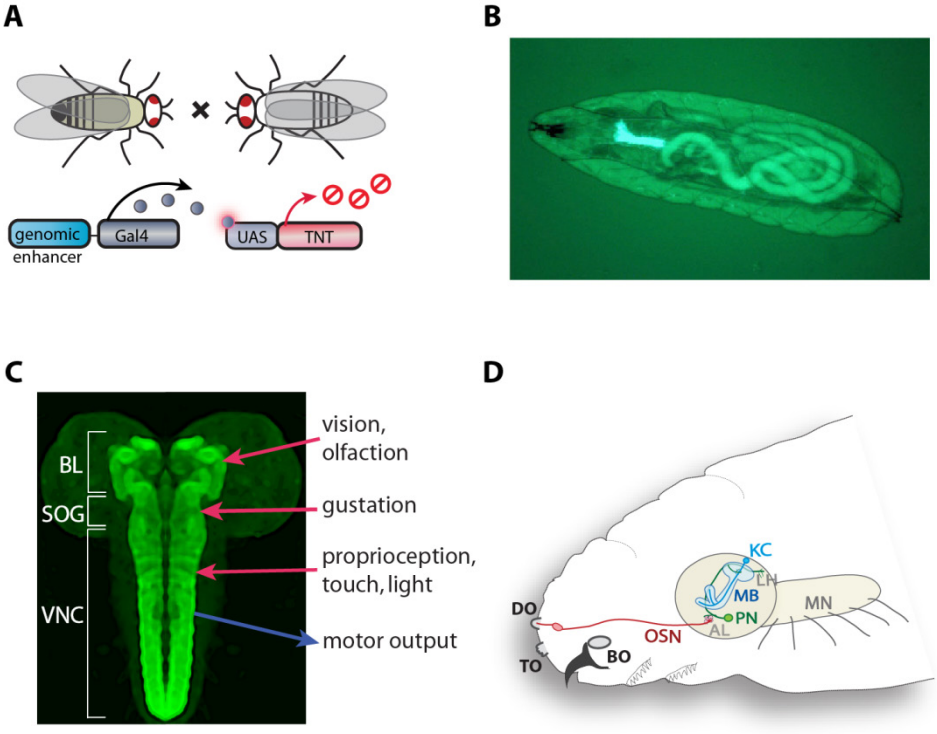

Figure 1.1: *Drosophila melanogaster* as a model organism for neurobiology
A: 3rd instar *Drosophila melanogaster* larva expressing GFP in the nervous system. The strongly labeled brain is located anterior, between mouth hooks and stomach. **B**: Rendered third instar central nervous system (CNS). Light green: neuropil as revealed by nc82 antibody labeling. The CNS is subdivided in 3 parts: brain lobes (BL), suboesophageal *ganglion* (SOG) and ventral nerve chord (VNC). Visual and olfactory information are conveyed to the BL, gustatory to the SOG, touch light and pain to the VNC. Motor output is created in the VNC. **C:** Gal 4 expression system: A female transgenic fly harboring the yeast transcription factor Gal4a under the control of a fly genomic enhancer is crossed to a transgenic male with a gene of choice (e.g. TNT) under the control of UAS. In the heterozygous offspring Gal4 drives expression of TNT. **D:** Olfactory system of the larva. Red: olfactory sensory neurons (OSN), green: Projection neurons (PN), blue: Kenyon cells (KC). AL: antennal lobe, LH: lateral horn, MN: motor neurons, DO: dorsal organ, TO: terminal organ, BO: Bolwig's organ

Targeted manipulation and monitoring of neural activity

Although invertebrate neurons show differences with those of vertebrates (e.g. lack of myelination), the basic principles of neural information transmission are conserved between species. Unstimulated neurons have a polarized membrane which is kept at a resting potential of approximately -70 mV. Excitatory presynaptic factors (like neurotransmitters or activation of sensory receptors) elicit calcium influx through cation channels. This in turn causes the voltage dependent ion channels to open and the membrane to depolarize. In a similar way inhibitory synapses cause hyperpolarization of the postsynaptic neuron. After initial depolarization influx of positively charged ions results in an action potential which propagates through the dendrite to the axon of the neuron, leading to Ca^{++} influx at the axonal presynaptic sites and neurotransmitter release from synaptic vesicles. Several agents have been employed in *Drosophila* to interfere with or to control the release of neurotransmitters. Using the UAS-Gal4 expression system, ion channels changing the membrane potential or toxin proteins inhibiting the vesicle release at the synapse can be targeted to specific neurons thus altering or impairing their activity cell autonomously.

Just as controlling the neural activity, monitoring a neuron's activity in response to a stimulus can be insightful to understand its function. Electrophysiology was used for decades to record the spike trains of invertebrate neurons; however, the technique is limited by the accessibility of the neurons to a recording electrode. Only recently recordings from central adult drosophila neurons could be performed successfully (Wilson, Turner et al. 2004). Especially given the smaller size of the larval neurons compared to e.g. mammalian or even adult

Drosophila, a less invasive technique would be desirable. Fortunately, during the last years genetically encoded calcium indicators (GECIs) have been developed. These proteins indicate calcium influx, and thereby its activity, by a change in fluorescence (Hires, Tian et al. 2008). In this way one can qualitatively and quantitatively determine neural responses in a non-invasive manner. Considering the transparency of the *Drosophila* larva, it represents an ideal model organism for applying this technique (Xiang, Yuan et al. 2010).

In our study we focused on two sensory modalities eliciting specific behaviors: electrotaxis and chemotaxis. While *Drosophila melanogaster* electrotaxis is described here for the first time, chemotaxis was studied for several decades leading to a clarification of the molecular basis and the first 3 layers of neural integration (Hallem and Carlson 2006, Leinwand and Chalasani 2011) (Figure 1.1 D). Most of the peripheral sensory system of the larva resides in cephalic sensory organs: the Dorsal Organ (DO, mostly olfactory neurons), Terminal Organ (TO, gustatory and cold sensation) and the Bolwig's Organ (vision) (Figure 1D). 21 olfactory sensory neurons located in the DO detect a wide range of chemical cues via olfactory receptors, which are then conveyed to a set of projection neurons located in the central brain lobes. The site of this first synapse is the antennal lobe. It comprises the axons of the sensory neurons (primary neurons) and projection neurons which convey the sensory information to further parts of the brain. Furthermore, local interneurons interconnect primary and secondary neurons (Chou, Spletter et al. 2010). The antennal lobe is known to be an integration center for chemosensory information, playing a key role in gain control and odor quality discrimination (Wilson, Turner et al. 2004). The projection neuron

axons project to higher brain centers; first synapsing onto Kenyon cells in the calyx of the Mushroom Body , then terminating in an area loosely described as the 'lateral horn'. There they connect with dopaminergic neurons (Wang, Pu et al. 2013) and probably further yet unknown cells. Kenyon cells are essential for memory and learning. Most likely they do not directly control innate behavior output, but rather modify it on a larger timescale of several minutes (Pauls, Selcho et al. 2010). Further neurons leading downstream to the motor output neurons located in the ventral nerve cord are yet unknown.

Taxis behavior

The behavior elicited by the integration of chemical sensory cues is named chemotaxis, which serves to locate the source of an odor cue (Figure 1.2A). Orientation in a graded chemical environment is a basic function for most species from single cells to plants to mammals. It's most primitive implementation can be observed in orientation towards nutrients by single-celled prokaryotes. In organisms with a nervous system specialized sensory cells and circuits for chemotaxis have evolved.

To infer the direction of a stimulus, animals commonly move their sensors in a search pattern and the underlying strategy and use of the sensors varies in different species (Gomez-Marin and Louis 2012). Over the past few years, the *Drosophila melanogaster* larva has become as a powerful model system for studying chemosensation (Gerber and Stocker 2007). Although chemotaxis can be positive and negative (attraction and repulsion), almost all odors elicit robust attraction in the larva. This reflects- alike the reduced complexity of the brain - the ethological purpose of the larval stage. It developed for a simpler set of tasks then the

adult, namely locating food and feeding, subsequently pupating after passing a critical body weight threshold (Truman and Riddiford 1999). Recently, the navigational strategy underlying larval chemotaxis was described in greater detail. It was shown that the larva employs a complex orientation strategy (Gomez-Marin, Stephens et al. 2011), clearly distinct from the chemotaxis observed in bacteria which rely on a biased random walk. In bacteria tumbling is decreased and swims are elongated when stimulus concentrations increase. However, the direction of both modes is random, only the frequency is modified by the environmental change. In contrast, larval taxis is based on the comparison of stimulus intensity over time, both during directed runs and the intermitted active sampling episodes (Figure 1.2B). Reorientation (turn episodes) is based on a decision inferred by recent sensory experience (Gomez-Marin, Stephens et al. 2011).

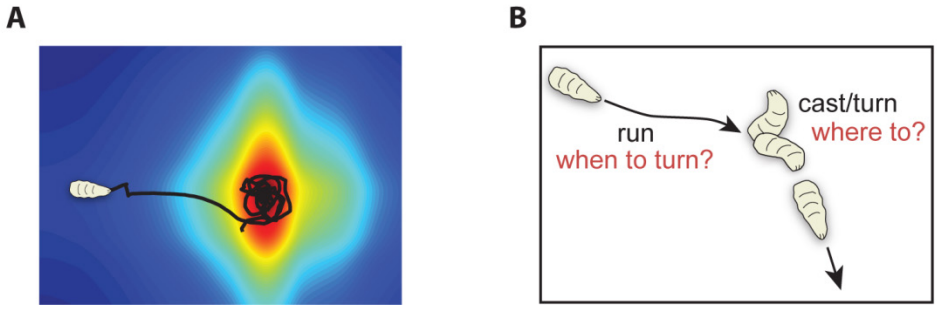

Figure 1.2: Larval Chemotaxis A: Illustrative trajectory of a wild type larva approaching and circling under a single odor source**. B:** Behavior modes implicated in chemotaxis: a run is interrupted by a cast/turn event. After sampling, the animal chooses a new run direction

Given the more complex layout of the behavior, we assumed that there must be specific neurons for controlling its different modes and their appropriate execution. Since we know that the larva performs behavioral decisions based on sensory experience, we hypothesized that for example, approaching an odor source must involve a form of memory storing information about the conditions a few seconds into the past and/ or an "integrator" which determines the change of the stimulus: is the odor becoming more or less intense, i.e. the slope of the gradient positive or negative? Likewise, this information must be used further downstream to control the motor output accordingly: steering the foraging or initiating a sampling and turning maneuver. The aim of this study was to identify neurons necessary for forwarding and integrating the sensory information. Finding yet unknown parts of the neural pathway underlying chemotaxis behavior, most likely downstream the projection neurons.

Behavioral screen

To that aim we employed a screening strategy recently used to identify neurons essential for various behaviors (Gordon and Scott 2009, Gong, Liu et al. 2010).The applied technique allows to directly probe the function of genetically defined neurons: A multitude of candidate Gal4 lines are crossed with a UAS-transgene that silences neurons (i.e. blocking neurotransmitter release, inhibiting spiking or even killing the cells) and progeny are screened for defective behaviors. Accordingly, we screened a collection of more than 1000 neural Gal4 lines. Using the UAS/Gal4 system to express tetanus toxin we abolished neurotransmitter release in different subpopulations of neurons and quantified its impact on chemotaxis behavior.

Equally, we intended to find the neural basis of orientation in a uniform electric field. Electrotaxis is found in many organisms and motile cells, including C. elegans (Gabel, Gabel et al. 2007), bacteria (Adler and Shi 1988), fungi (Gow 1994), amoeba (Korohoda, Mycielska et al. 2000), the slime mold *Dictyostelium discoideum* (Sato, Ueda et al. 2007) and neuronal growth cones (McCaig, Rajnicek et al. 2005). However, hitherto it was not described for *Drosophila melanogaster*. We found that larvae robustly approach the cathode when exposed to a static and uniform electric field generated by two electrodes (Figure 1.3). Making use of the available genetic tools and detailed behavioral analysis, we aimed at achieving a detailed description electrotaxis in the larva. Finally our screen allowed us to explore which neurons are responsible for eliciting or controlling this novel navigation behavior.

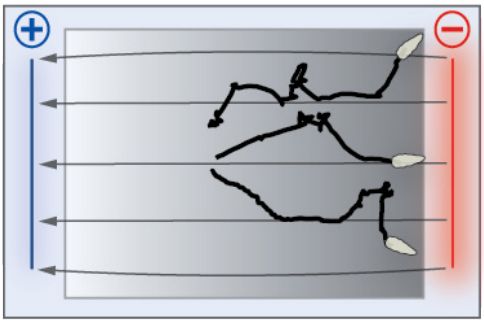

Figure 1.3: Drosophila larval electrotaxis. An agarose surface (foraging substrate) is located between two electrodes of opposite polarity (blue and red bar). Black lines: 3 illustrative trajectories of larvae navigating towards the cathode. Grey Lines: electric field lines

Chapter 2:

Behavioral screen to identify neurons underlying chemotaxis and electrotaxis

2.1 Abstract

Navigation behavior is critical for the survival of most species, underlying fundamental aspects of life such as finding food or locating a mate. We were investigating this problem in the larval *Drosophila melanogaster* nervous system, which shares basic structural similarities with its adult counterpart, while being strongly reduced in number. Larval taxis represents a powerful model to gain a more systematic insight into the anatomical and functional layout of the circuits underpinning orientation behavior. It comprises precise detection of changes in cue intensity, sophisticated central processing of sensory inputs and a set of distinct behaviors such as forward locomotion, head casting and turning. This allows the animal to effectively orientate in a gradient environment. Whereas the first and second-order olfactory neurons are relatively well characterized, our understanding of the downstream neurons integrating dynamic olfactory information remains poor. Moreover, we describe navigation in an electric field (electrotaxis) as a novel larval taxis behavior for the first time. Until now nothing was known about the neurons responsible for detecting and reacting to electric fields.

In order to identify neurons underlying orientation behavior, we have undertaken a large behavioral screen testing the performance of larvae in both behavioral paradigms: chemotaxis and electrotaxis. The Gal4-UAS binary expression system was exploited to genetically silence targeted neural populations of the larval brain. More than 1000 GAL4 enhancer trap driver lines were crossed with a UAS reporter expressing tetanus toxin (TNT) that effectively silences neuronal activity by impairing synaptic transmission. The functional consequences of these

losses of function were assessed in a set of motility and chemotactic assays. Behavioral performances were quantified by an automated statistical analysis, which yielded an unbiased scoring of all phenotypes and resulted in over 100 candidate lines for further investigation.

2.2 Introduction

In order to identify neurons involved in chemo- or electrotaxis we performed a large behavioral screen, testing the effect of silencing subpopulations of the brain on larval behavior. To this aim we used a collection of neural Gal4 driver lines (NP lines) created by the DGRC consortium to drive a synaptic inhibitor in genetically defined populations of neurons (Hayashi, Ito et al. 2002). The NP enhancer trap lines were created by mobilizing a P[GawB] element. The respective regulatory elements of each insertion site (promoters) thus controlling Gal4 expression. Of each line rough expression pattern in the adult fly and the gene(s) affected were known. As an effector protein we used tetanus toxin light chain (TNT), an extremely potent neurotoxin produced by the vegetative cell of *Clostridium tetani* (Gill 1982, Sweeney, Broadie et al. 1995). Tetanus toxin interferes with the machinery needed for vesicle release at the synapse, proteolytically cleaving synaptobrevin, one of the core constituents of the vesicle fusion complex. As a consequence, synaptic transmission relying on transmitter release is abolished while leaving the neuron alive and capable of eliciting action potentials. Importantly, it was shown that expression of TNT effectively interferes with neural activity, yet it does not perturb cell survival, differentiation, axonal outgrowth or morphological synaptogenesis (Sweeney, Broadie et al. 1995). As it is reported to be a very powerful toxin (Gill 1982), its silencing potency is less affected by varying expression levels.

In order to reliably detect lines which were affected in their behavioral output, we designed 3 types of larval behavior assays. In a first set of experiments we tested healthy third instar larvae for normal

locomotion. In parallel, chemotaxis was probed by testing the approach of an odor source. In a third assay we tested electrotaxis-performance. Wild type larvae exposed to a uniform electric field robustly approach the cathode. Making use of a novel behavioral electrotaxis arena (details see Material and Methods), we tested for lines being deficient in navigating along an electric field.

As readout, we combined the experimenter's observations with unbiased computer-vision quantification. We monitored the assays with a camera and quantified the behavior with custom made image-analysis software and a statistical test for differentiating wild-type-like behavior from mutants. The underlying rationale was to find lines which showed robust taxis defects without being affected in there foraging behavior.

2.3 Materials and Methods

Fly stocks

Fly stocks were raised on standard cornmeal medium at 18 °C on a 12h:12h day-night cycle colored with bromophenol blue. This method greatly improved the resolution when tracking groups of larvae. The larvae were shifted to room temperature for testing temperature at least 3 hours before conducting the behavioral tests. For the screen a selection of 1118 fly lines from the NP collection was used (Hayashi, Ito et al. 2002). Effector lines: w;UAS-TNTE;+ (II), UAS-mcd8GFP. Other Gal4 insertion lines used were: Orco-Gal4 (Wang, Wong et al. 2003), 109(2)80-Gal4 (Grueber, Jan et al. 2002). As a wild type control we used a heterozygous cross of UAS-TNTE with w1118.

Behavioral assays:

For all assays 1.5 % agarose (Seakem-LE, Lonza) prepared with deionized water was used. Larvae were gathered from the food in 15 % Sucrose and washed in deionized water before placing them in the test arena. In each arena ca. 15 animals were tested. For all assays we performed minimum n=2 experiments.

Locomotion assay: On a custom made plate fix mounted on a white back light (Kaiser Slimlite) 2 fresh standard petridishes (90 mm diameter, Fisher Scientific) filled with 1 cm high agarose were placed for each experiment. Larvae were introduced in the middle each petridish and free foraging was monitored for 3 min.

Chemotaxis assay: On a custom made plate-fix mounted on a white back light we placed 2 fresh standard petridishes filled with 1 cm high Agarose. A small disk of filter paper (5-mm diameter) was soaked in an

aqueous solution of 1-hexanol 60 mM (CAS: 111-27-3, 98% pure, Sigma-Aldrich). The disk was placed at the center of the dish and the larvae were introduced approximately 2-cm away from it. The gradient odor gradient established while harvesting the larvae. Larvae were introduced in the middle between the odor source and the dish border and were monitored for 3 minutes.

Electrotaxis assay: Two platinum electrodes lined the sides of a Plexiglas chamber (33 x13,5 cm) which was filled with deionized water. A platform supported an agar slab, held by a casting tray, resulting in a 25 x 13 cm behavioral arena semi-immersed in the water. The apparatus was placed on a white back light for illumination (Kaiser Slimlite). Ca. 15 animals were introduced in the middle of the arena and their behavior monitored for 3 minutes. The voltage was applied via a custom power supply which was controlled by custom-made Matlab software, controlling in parallel camera acquisition and voltage level.

Behavior quantification:

In all assays larvae were monitored with a CCD color camera (Basler, scA1390-17fc). The cameras were controlled via Matlab Image Acquisition Toolbox and a custom made Matlab (The Mathworks) image analysis software. Pictures were taken every 10 seconds, and the position of each animal and subsequently the median distance of all animals from the arena center was calculated for each time point. For statistical analysis of the results we created a reference set of behavioral experiments, comparing wild type behavior with 2 benchmark lines. For chemotaxis we silenced the olfactory sensory neurons using Orco Gal4>UAS-TNT, resulting in anosmic larvae, for locomotion we silenced the multidendritic neurons which are essential for proper forward crawling using 109(2)80-

Gal4>UAS-TNT. For each genotype we performed 10x2 experiments. We determined the 3 time points which showed the lowest p-values when tested with a Wilcoxon rank sum test. Using this dataset we also determined an appropriate alpha-value for differentiating wild type from aberrant behavior (10-6 for locomotion and 10-4 for chemotaxis).
As a condition for a line being a "hit" we established a significant difference based on the Wilcoxon test versus the reference set for 3 consecutive time points: 120, 130 and 140 seconds into the experiment for locomotion and 150, 160 and 170 seconds for chemotaxis in both arenas.
Since there was no mutant for electrotaxis known, we compared the mean distance to the center of wild type and each tested line for the last 3 time points (160, 170, 180 seconds).

Histology:

The larval central nervous system and the peripheral chemosensory organ (dorsal organ, DO) were dissected and fixed in 4% formaldehyde in phosphate buffered saline(PBS) for 30 minutes at room temperature. After 3 x rinsing in PBS+0.2% Triton-X the tissue was blocked for 30 minutes in 3% goat serum in PBS-TX. The primary antibody was incubated over night at 4°C. After 1x10 min rinse and 2x 2h or longer, the tissue was incubated with the secondary antibody in PBS-TX at 4°C over night. After 2x 10 min rinse in PBS TX the CNS and the DP were mounted in Vectashield mounting medium (Vectorlabs) on lysine covered cover slips. Imaging was performed with a Leica TCS SPE confocal microscope.

antibody	*source*	*dilution*
Nc82-s (bruchpilot)	Developmental Studies Hybridoma Bank	1:30

GFP	Invitrogen	1:500
Texas Red Goat Anti-mouse	Jackson Immuno Research	1:500
FITC Goat Anti-rabbit igG	Jackson Immuno research	1:500

2.4 Results

2.4.1 Behavioral tests

From the DGRC Gal4 collection we selected about 1300 lines located on the second or third chromosome. The first chromosome (X or Y) was neglected, as it is difficult to work with, and possibly leads to sex specific effects. Moreover, we rejected lines showing very broad expression in the adult stage. Out of 1623 NP Gal4-lines 1122 were homozygous viable and crossed to UAS-TNT flies. From these crosses 219 didn't develop to healthy 3rd instar larvae and were discarded. Finally, 903 lines were tested in the behavioral assays for defects in locomotion, chemotaxis and electrotaxis (Figure 2.1A). We obtained minimum n=2 for each genotype. After automated quantification and statistical analysis (Figure 2.1B) we obtained 403 lines showing no phenotype (Figure 2.1C) and 262 lines with a distinct locomotion deficit in many cases also leading to a chemotaxis or electrotaxis deficit. Since we were interested in integration of sensory signals but not in mere locomotion deficiencies hampering the navigation, these lines were not further analyzed. In the chemotaxis assay 202 lines were found altered specifically without having apparent locomotion impairment. The electrotaxis assay yielded 36 deficient lines. 16 of those showed impairments in both chemotaxis and electrotaxis behavior. The lines qualified as hits without strong locomotion deficits were confirmed visually by reviewing the raw data (pictures) and the notes of the experimenter. Eventually, we chose 114 lines showing a chemotaxis deficit for anatomical assessment. 36 electrotaxis deficient lines were

chosen for retesting in the electrotaxis assay to confirm the phenotype and subsequent anatomical assessment.

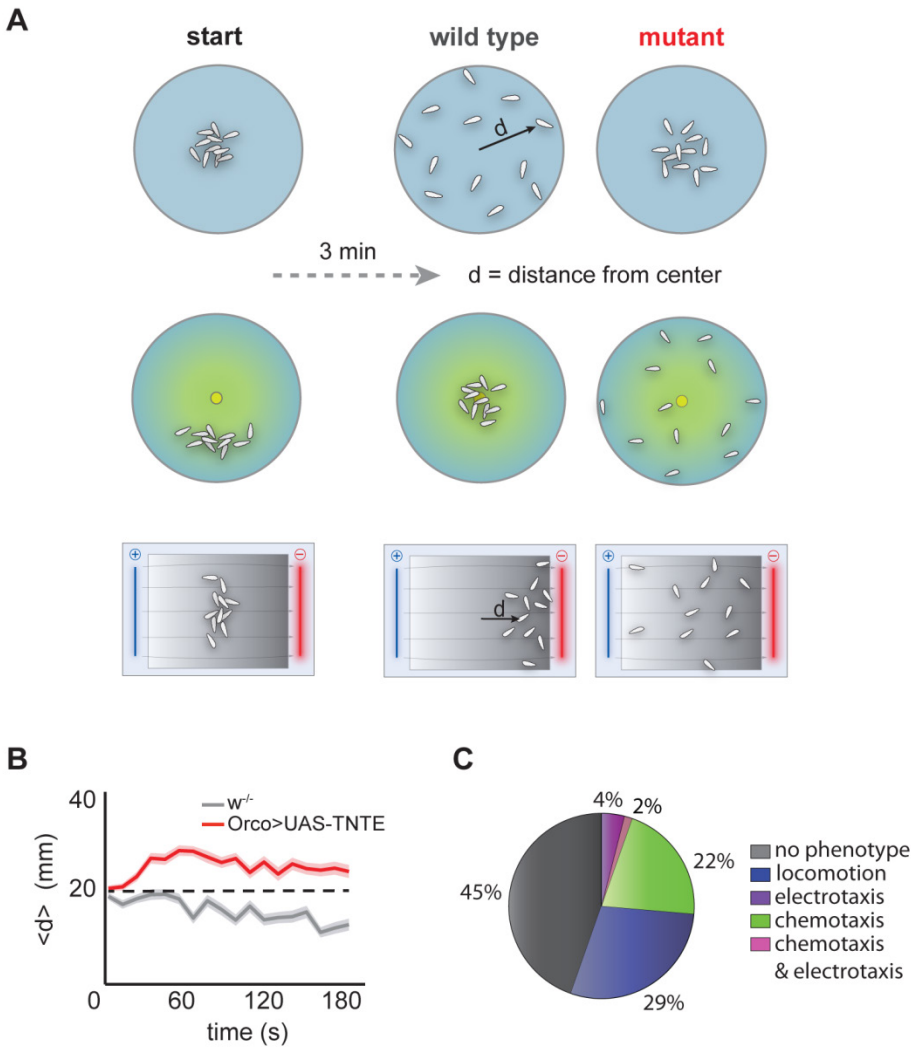

Figure 2.1: Primary behavioral screen **A:** Behavioral assays used for the primary screen: locomotion (top), chemotaxis(middle) and electrotaxis(bottom). **B:** Quantification of mean distance over time of larvae based on benchmark data set: red: anosmic larvae, grey: wild type. **C:** Frequencies of phenotypes found in the primary screen. Phenotype class frequency is indicated as percentage of all (903).tested lines

2.4.2 Anatomy:

In order to determine which neurons have been silenced in the lines qualified as taxis deficient, we performed immunstainings on flies expressing membrane-targeted green fluorescent protein mcd8-GFP, under control of the respective driver lines. As a reference for anatomical annotation we also labeled bruchpilot, a presynaptic protein which reveals the complete functional neuropil and thus anatomical hallmarks of the larval brain (for example the antennal lobe or the mushroom body). We examined the central nervous system and the anterior chemosensory organ (dorsal organ, DO). The rationale was to discard lines which showed expression in the olfactory sensory neurons and/or the majority of projection neurons, as silencing these cells evidently causes a loss of chemotaxis ability. We also assessed expression in the Kenyon cells, since we found in preliminary experiments that expressing TNT in these cells continuously throughout development caused a notable chemotaxis deficit.

In total 127 lines were labeled and imaged. Out of those 13% showed expression in the olfactory sensory neurons (OSN) and 2% in a large number of projection neurons (PN). As mentioned before, these lines were discarded since the silenced first and second order neurons were the cause of the deficiency. We also classified the expression patterns as being “busy” (many neurons labeled, e.g. NP 2814,Figure 2.2

left panel) or sparse (less than approximately 2 dozen cells per hemisphere labeled, e.g. NP 1613 Figure 2.2, right panel). While establishing our behavioral paradigms we found that complete silencing of the mushroom body throughout development itself leads to impaired chemotaxis. For further testing we therefore focused on sparse lines, preferably with no or little covering of the Kenyon cells.

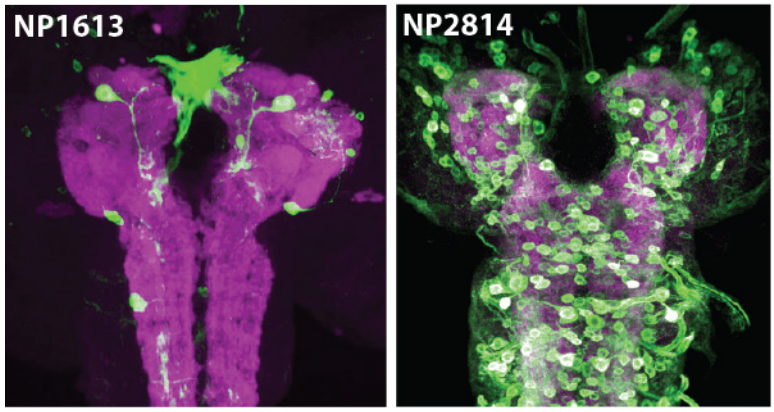

Figure2.2: Examples of range of neurons covered by NP lines Left panel: sparse line, NP1613>UAS-mcd8GFP. Right panel: "busy" line, NP2814>UAS-mcd8GFP. green=anti-GFP, magenta=anti-nc82

2.5 Discussion

Orientation behavior in gradients is vital to animals from bacteria to mammals. *Drosophila* has emerged as a premiere model system to study the neural basis of behavior, specifically the sensorimotor transformation directing orientation. Throughout the last four decades genetic screens in Drosophila have identified many genes involved in neural development and function, e.g. by the groundbreaking works of Seymour Benzer and Nüsslein-Volhard and colleagues among many others (Benzer 1967, Nusslein-Volhard and Wieschaus 1980). However, until recently it was impossible to directly monitor or interfere with the function of neurons in an intact animal. This has changed in the past few years with the development of a range of new tools for measuring and manipulating neural activity in the fly, making it now possible to specifically perturb neural circuits. Here, we made use of these tools to identify central neurons underlying taxis behavior in the *Drosophila* larva. We screened a large collection of Gal4-lines driving a synaptic silencing toxin in distinct subsets of neurons, assessing the effects on chemotaxis and electrotaxis. Interestingly, only 6% of these lines didn't produce apparently healthy third instar larvae apt for testing. This confirms on the one hand our strategy of preselecting against very busy adult expression and on the other hand it suggests general weak developmental effects of silencing neurons using tetanus toxin. We found an altered behavior in 55% of the tested lines. Besides automated quantification we also qualitatively assessed the phenotype, taking into account the experimenters observations while performing the experiments. Unexpectedly, we didn't observe extraordinary behaviors, being

extremely different from the normal behavioral repertoire of a larva. One could argue that the larval neural system has developed to produce a restricted set of motions and therefore not even severe manipulation would not create behaviors completely different from those described so far. Nonetheless, we reckoned that our intervention in the function and maybe also wiring would lead to strongly aberrant behaviors (e.g. exclusively crawling backwards). However, we cannot rule out that given the quite general metric used in the primary screen, some behavioral features were not captured by thee experimenter and therefore overlooked. Another reason may be that strong behavioral alterations cause lethality in early larval stages. Generally, the amount of lines being specifically altered in chemotaxis behavior (114 out of 903 tested) seemed high enough to comprise a range of different neural subsets underlying its proper execution.

The electrotaxis behavior assessment was even more general, given the lack of any previous description of the behavior. We selected all lines showing a reduced performance of approaching the cathode. We were excited to find more than 30 lines impaired in electrotaxis but not in locomotion nor in chemotaxis. In fact, there were only 8 lines impaired in both taxis types, 3 of them showing a very broad expression pattern, hinting at a general effect on brain function. This result suggested a separate neural implementation of this behavior, apart from other sensory modalities. The numbers of neurons in these lines was generally exceeding 2 dozen cells, in some case apparently covering a very large population of cells. This evoked the curious question how a larva with maybe a third of its neurons silenced can actually still develop and behave quite normally. Of course, given the rather superficial anatomical

assessment in the primary screen set, we didn't exclude secondary neurons: cells which develop throughout larval stages but are non-functional until after pupation. This might have led to an overestimation of covered neurons. Taken together, the primary screen resulted in a promising pool of more than 100 lines for further analysis.

Chapter 3:

Chemotaxis secondary screen – Identifying a neural population underlying chemotactic behavior organization

3.1 Abstract:

In a large behavioral screen silencing subpopulations of neurons in the larval brain, we identified more than 100 candidate lines defective in chemotaxis. After anatomical assessment of the affected neurons and a high-resolution behavioral quantification we selected a Gal4 line covering a small population of neurons and specifically affecting chemotaxis performance: NP4820. Detailed behavioral analysis revealed the nature of the defect as an impairment of timing of behavioral transitions in respect to sensory experience. Runs were strongly prolonged, cast/turn episodes were ill-timed and their execution altered. Accordingly, activating the neurons with a heat-responsive ion channel was sufficient to initiate cast/turn maneuvers. Applying an intersectional strategy we could map the neurons underlying the phenotype to the suboesophageal ganglion (SOG), which was known so far as a region for gustatory sensory processing. Using phototaxis as a second behavioral paradigm we could show that the phenotype is generalized over sensory modalities. We therefore conclude that suboesophageal ganglion hosts a group of neurons controlling the transition from run to cast/turn. As this function pertains to the processing of inputs from different sensory modalities, we argue that the SOG — a center traditionally associated with gustation — operates as a general controller circuit that converts changes in sensory stimulus into the selection between alternative behavioral programs or actions.

3.2 Introduction:

While tracking an appetitive odor, organisms seek to navigate through a gradually changing sensory environment, eventually reaching the odor source. To this end, different species implemented different strategies. While Bacteria- like *Escherichia Coli*- and the nematode *Caenorhabditis elegans*, rely on a random walk biased by sensory experience (Pierce-Shimomura, Morse et al. 1999, Shimizu, Tu et al. 2010), animals with more complex nervous systems show refined scent-tracking strategies. Dogs for example, hunt their prey by moving their nose back and forth across an odor trail and rats use stereo snapshots of the environment making discrete sniffs(Thesen, Steen et al. 1993, Rajan, Clement et al. 2006).

Recently it was shown that the *D. melanogaster* larva chemotaxis cannot be explained neither by a simple biased random walk, nor stereo sensation. It rather employs an active sampling strategy, which corresponds to klinotaxis: a single sensor infers the chemical environment by sequential sampling and comparison (Gomez-Marin, Stephens et al. 2011). Larvae do this by two distinct modes of behavior: runs and cast/turn (Figure 1.2). While crawling through an odor landscape the animal is engaged in forward runs. During a run, an increasing or decreasing odor gradient is detected keeping the animal in the running mode. A decline in odor concentration is triggering the animal to stop and actively sample its environment by head sweeps. By this cast/turn episode a new foraging direction is chosen, improving the alignment of the animal towards the odor source.

The mass assays used in the primary screen were designed to test for the general ability of the animals to locate and stay under an odor source. However, it did not allow us to identify which specific parts of the chemotaxis behavioral algorithm are altered. We therefore performed a second set of experiments to detect more subtle defects. Making use of a high-resolution computer-vision algorithm recently developed in the lab, we quantified the behavior of single freely moving larvae in a defined odor gradient. Assessing the anatomy of the silenced neurons we aimed to attribute the behavioral defect to a particular population of neurons and to establish an admissible hypothesis of the neuron's function and the kind of "computation" they perform. In fact, for most fly behaviors we have little or no knowledge on what interneurons are involved. For somatosensory, auditory and some gustatory behaviors only the peripheral sensory neurons are known. Only recently neural populations could be identified underlying courtship behavior (Clyne and Miesenbock 2008), the proboscis extension response to sugar (Gordon and Scott 2009, Marella, Mann et al. 2012) and phototaxis (Gong, Liu et al. 2010).

Olfactory integration has been studied extensively throughout the last two decades, revealing not only the peripheral neurons and their odorant receptors, but also secondary (projection neurons) and third layer neurons (Kenyon cells, lateral horn neurons). However, further yet unknown neural pathways must convey the olfactory signal to the ventral nerve chord producing an appropriate behavioral response. The Gal4 lines identified in our primary screen potentially labeled these neurons. They were likely either cells which directly feed forward the sensory information toward motor neurons , or on the other hand, modulating it, i.e. influencing type or strength of the output. For the sake of feasibility,

we eventually focused on the line NP4820-Gal4, as it showed a pronounced and robust phenotype, while covering a considerable small number of neurons. Making use of the experimental toolkit for *Drosophila melanogaster*, we could show that NP4820 comprises a group of neurons controlling the onset and execution of cast/turn episodes of taxis behavior.

3.3 Material and Methods:

Fly stocks:

The lines selected from the primary screen originated from the NP collection available from the *Drosophila* Genetic Resource Center in Kyoto (Hayashi, Ito et al. 2002). The following stocks were used: w;UAS-TNTE;+ (Sweeney, Broadie et al. 1995) , w;*Orco*-Gal4;UAS-mcd8GFP (gift from L. Vosshall), P[GawB]109(2)80-Gal4 (Grueber, Jan et al. 2002), w;+;*Orco*^{2} (Larsson, Domingos et al. 2004), w;*tub*-Gal80ts;+ (McGuire, Mao et al. 2004), w;UAS-dTrpA1;+ (P. Garrity, (Hamada, Rosenzweig et al. 2008)), w;*tsh*-Gal80;+ (gift from the Simpson lab), w;+; *Cha3.3*-Gal80 (Kitamoto 2002), *elav*-Gal4;+;+ (stock# 458, Bloomington Stock Center).

Histology: see chapter 2

Image rendering: performed with Imaris software (Bitplane Scientific Software).

Secondary screen assay: We adapted a machine-vision algorithm previously described in ref. (Gomez-Marin, Partoune et al. 2012) to track single larvae in a small rectangular arena coated with agarose. The arena was set up as a single-odor-source assay (Louis, Huber et al. 2008) to test single larvae at a time. The odor source was placed out of reach of the larva. The two odors tested were 1-hexanol and ethyl butyrate (CAS: 105-54-4, Sigma-Aldrich) dissolved in paraffin oil (Sigma-Aldrich). The tracking of individual larvae was achieved with a CCD camera (scA1390-17fc, Basler) that acquired images at a frequency of 0.2 Hz.

Gradient Quantification: Following the procedure described in ref. (Louis, Huber et al. 2008), odor profiles were measured at fixed positions

on the plate using a FT-IR spectrometer (Tensor 27, Bruker). We calculated the absolute concentration of odor in gaseous phase upon application of the Beer-Lambert law ($A = \varepsilon \times l \times C$) where A denotes the absorbance, ε the molar extinction coefficient, l the length of the section considered and C the average concentration along this section. Molar extinction coefficients were estimated in gaseous phase with a standard gas-flow cell (ε1-hexanol=140 M-1cm-1 at 2940 cm-1 and εethyl butyrate= 315 M-1cm-1 at 1758 cm-1). Due to the limited sensitivity of the spectrometer, the landscapes of the odor gradients could not be directly measured at the source concentrations that were used in the behavioral experiments. We inferred the experimental landscapes by scaling down the gradient reconstructed at the lowest source concentration possible (ethyl butyrate: 30 mM and 1-hexanol: 500 mM).

Behavioral analysis for the secondary screen: Behavioral data was classified as described in (Gomez-Marin, Stephens et al. 2011, Gomez-Marin, Partoune et al. 2012). To analyze the data shown in Figures 2.1-2.5, we introduced an additional set of metrics: the percentage of time spent in a quadrant of 2x2 cm centered on the odor droplet. To calculate the persistence duration — a metric equivalent to the persistence length (Bednar, Furrer et al. 1995) — we computed the difference between the heading angles ($\Delta\alpha$) at a time point of reference and for consecutive time points (t) along the trajectory. To account for differences in speed between genotypes, the time series $\Delta\alpha(t)$ was normalized by the average distance travelled during a trajectory. As for other systems characterized by their persistence length (e.g., the rigidity of polymers like DNA or that of spaghettis), we observed that the time series $\cos(\Delta\alpha(t))$ follows an exponential decay. After averaging the time series $\Delta\alpha(t)$ over every

possible start position and trajectory, the persistence duration P was estimated from a least-square fit using the relationship <cos(Δα(t)> = e^-(t/P) where <> denotes the average over all start positions and trajectories.

Gain of function manipulations: Gal4 driver lines were crossed to UAS-dTrpA1. As a negative control, we used $w^{-/-}$ x UAS-dTrpA1. As positive control we used pan-neural *elav*-Gal4>UAS-TrpA1, which leads to complete paralysis when globally activated. This cross was used for determination of the threshold temperature specific to our setup (data not shown). This temperature was determined to be about 28°C, in agreement with previous work (Pulver, Pashkovski et al. 2009). To activate the dTrpA1 effector, we subjected larvae to a gradual temperature increase in time. We placed a 1-mm thick layer patch of 1% agarose on the surface of an aluminum slab painted in black, which was connected to a 12 x 8 cm Peltier device (TE Technology). The temperature was controlled and logged by a commercial thermistor and software provided with the Peltier element (TE Technology). Unrestrained single larvae where monitored for 3 min. Ten seconds into the experiment, the temperature of the aluminum plate was raised from 24 to 31°C (0.12°C/s), yielding a temperature ramp of 23 to 29°C at the surface of the agarose substrate. The temperature of the aluminum plate was kept at 31°C for 30 s before it decreased back to 24°C at a rate of 0.12°C/s. Behavior was monitored using the same hardware and Matlab software as for the chemotaxis assay.

Phototaxis assay: To create light gradients with inverted Gaussian geometry, we used a blue LED with peak emission at 470 nm (PLS 0470-030-S, Mightex Systems). Single larvae were introduced on an agarose surface at the position corresponding to the minimum of the light gradient

and were tracked for 5 min. The position of the larva was monitored in real time and the light intensity was continuously updated according to a preset landscape. The light intensity at the agarose surface was determined with a photodiode and a benchtop amplifier (SM05PD7A and PDA200C, Thorlabs).

3.4 Results:

3.4.1: Secondary Screen:

Based on primary screen behavioral and anatomical assessment, we chose 56 Gal4 lines for retesting in a secondary screen. We excluded very broad expression patterns and lines showing expression in peripheral neurons or a large number of projection neurons, which is known to cause a chemotaxis deficiency. The lines were again crossed to UAS-TNTE and single animal chemotaxis behavior was tested in a controlled odor gradient with a 125 mM 1-Hexanol point source. Using our custom tracking software, we quantified the position and the body posture of the larva at 5 Hz throughout the navigation in the gradient. As a metric for general chemotaxis performance we applied the odor zone index, i.e. the fraction of time an animal spent in a defined region close to the odor source droplet. In addition, we calculated mean velocity and latency (time passed before first entering of odor zone). We obtained a variety of phenotypes ranging from nearly wild type behavior to strong phenotypes including complete smell blind larvae and pronounced locomotion anomalies (Figure 3.1A,B). Out of 56 retested lines we could confirm 42 as significantly different in chemotaxis performance from wild type or the parental TNT line quantified by the odor zone index (Table 1, Figure 3.1A).

Table1:
NP Gal4 –lines leading to a behavioral deficit in the secondary screen, quantified as an odor zone index significantly lower than wild type.

Genotype	# DGRC	odor zone index
positive control w-/- x UAS-TNTE		0,53
y[*] w[*]; P[GawB}NP0171 / TM6, P[UAS-lacZ.}	103547	0,30
y[*] w[*]; P[GawB}NP0423 / TM2	103614	0,43
w[*]; P[GawB}NP0756 / TM3, Ser[1]	103747	0,18
[*]; P[GawB}NP0845 / CyO	103786	0,02
w[*]; P[GawB}NP0908 / CyO	103813	0,12
y[*] w[*]; P[GawB}NP1273 / CyO, P[UAS-lacZ.}	103963	0,18
y[*] w[*]; P[GawB}NP1288 / CyO, P[UAS-lacZ.}	103968	0,34
y[*] w[*]; P[GawB}NP1326 / TM6, P[UAS-lacZ.}	103989	0,33
y[*] w[*]; P[GawB}NP1613 / TM6, P[UAS-lacZ.}	104050	0,43
w[*]; P[GawB}NP2002 / TM3, Sb[1] Ser[1]	104060	0,26
w[*]; P[GawB}NP2070 / TM3, Sb[1] Ser[1]	104076	0,35
w[*]; P[GawB}NP2144 / CyO	104104	0,26
w[*]; P[GawB}NP2554 / TM3, Sb[1] Ser[1]	104237	0,10
w[*]; P[GawB}NP3036	104350	0,36
w[*]; P[GawB}NP3040	104352	0,42
w[*]; P[GawB}NP3204	104411	0,35
w[*]; P[GawB}NP3456	104511	0,36
w[*]; P[GawB}NP3556	104539	0,26
w[*]; P[GawB}NP3596	104553	0,02
y[*] w[*]; P[GawB}NP4228 / CyO, P[UAS-lacZ.}	104638	0,38
y[*] w[*]; P[GawB}NP4236 / CyO, P[UAS-lacZ.}	104641	0,24
w[*]; P[GawB}NP4820 / CyO	104798	0,25
y[*] w[*]; P[GawB}NP5142 / CyO, P[UAS-lacZ.}	104870	0,07
y[*] w[*]; P[GawB}NP5297 / CyO, P[UAS-lacZ.}	104941	0,24
y[*] w[*] P[GawB}NP6328 / CyO, P[UAS-lacZ.}	105201	0,31
w[*]; P[GawB}NP0147 / CyO, P[UAS-lacZ.}	112062	0,38
w[*]; P[GawB}NP0754 / TM3 Ser	112315	0,40
w[*]; P[GawB}NP0925 / CyO;TM3 Ser	112401	0,35
y[*] w[*]; P[GawB}NP1559 / CyO, P[UAS-lacZ.}	112697	0,07
y[*] w[*]; P[GawB}NP1623 / CyO, P[UAS-lacZ.}	112736	0,18
w[*]; P[GawB}NP2009 / TM3, Sb[1] Ser[1]	112743	0,45
w[*]; P[GawB}NP2351 / CyO; TM3, Sb[1] Ser[1]	112896	0,06
w[*]; P[GawB}NP2526 / CyO	112951	0,47
w[*]; P[GawB}NP2566 / TM3, Sb[1] Ser[1]	112972	0,12
w[*]; P[GawB}NP2583 / CyO	112976	0,39
w[*]; P[GawB}NP3084	113094	0,20
w[*]; P[GawB}NP3182	113144	0,46
w[*]; P[GawB}NP4675 / CyO; TM3, Sb[1] Ser[1]	113495	0,07
w[*]; P[GawB}NP5159 / CyO, P[UAS-lacZ.}	113606	0,18
y[*] w[*]; P[GawB}NP6263 / CyO, P[UAS-lacZ.}	113885	0,12

We then reduced the number of lines of interest considering qualitative assessment of the phenotype, anatomy and phenotypic quantification obtained in the secondary screen. We ruled out additional lines because we failed to reproduce the phenotype (odor zone index not significantly different for wild type) or had only a very weak phenotype (e.g.1613, Figure 3.1Bvi). Other lines which showed a strong general chemotaxis phenotype (e.g. 2351, Figure 3.1Biv) or latency (e.g.2002, Figure 3.1Bv) had to be discarded because too many neurons were affected. Likewise we discarded lines when strong locomotion impairment was observed leading to very low mean velocity. For the remaining subset of 5 Gal4 lines we continued by testing the parental Gal4 driver lines in the same paradigm to rule out any effect of the insertion. This led us to abandon 2 more lines (e.g. 1559, 2144, Figure 3.1BI and 3.1Biii).

Finally, we decided to focus on the line NP4820, which resulted to represent the best trade-off between a striking phenotype and a relatively small neuron number in the brain lobes, SOG and VNC affected (Figure 3.1Bii, Figure 3.2A).

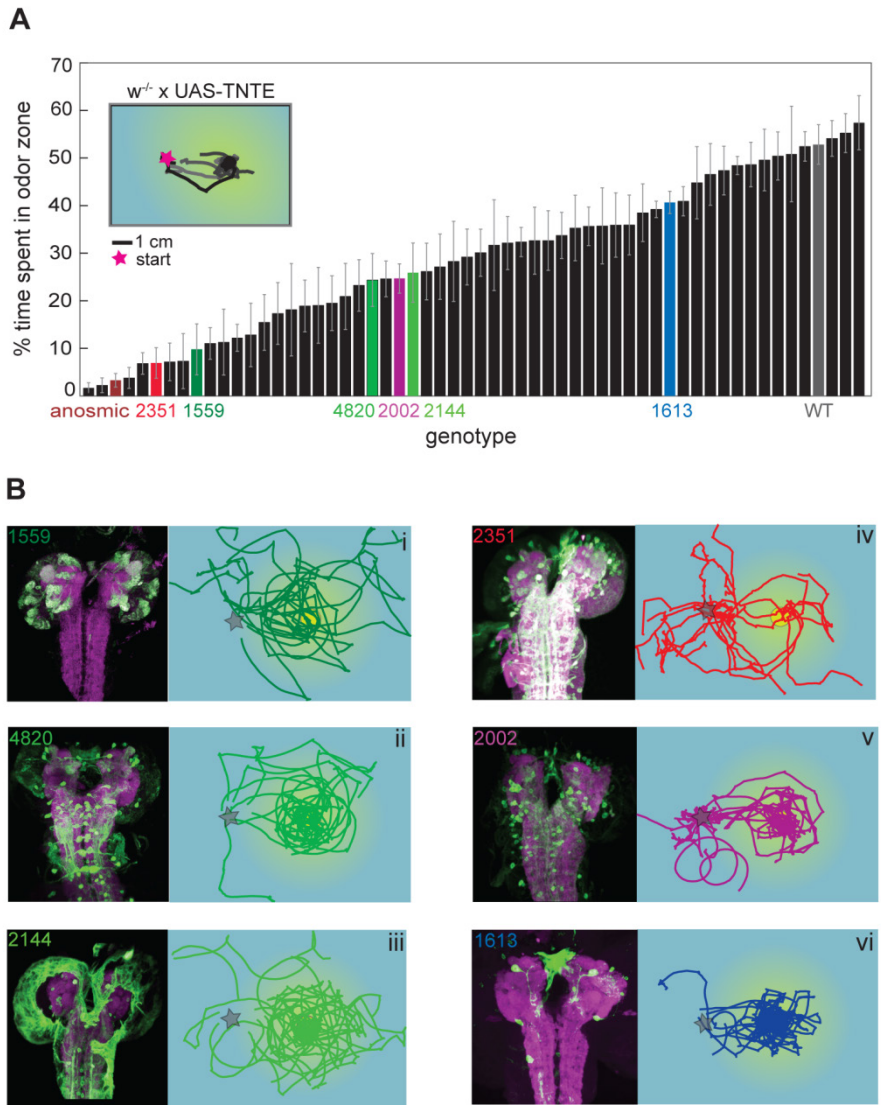

Figure 3.1: Secondary screen results A: Secondary screen based on a modified chemotaxis assay described in ref. (Louis, Huber et al. 2008) (inset). The behavior of the positive control is illustrated by 4 representative trajectories. Results of 57 tested lines with pure chemotactic defect sorted by performances. Bars show mean of the percentage time spent in the odor zone (N=15 trials); errorbars indicate the SEM. **B:** Six representative Gal4-lines showing chemotactic impairment when crossed to UAS-TNTE. The respective performance was quantified as indicated in (A). The left panels show the respective expression patterns in the larval central brain when crossed to UAS-mcd8GFP. The right panels show the trajectories of 4 animals corresponding to each illustrative Gal4 line. Green: anti-GFP, magenta:

anti-nc82 (neuropil marker). i-iii: 3 lines with a medium phenotype and sparse expression patterns. iv: strong phenotype and broad expression pattern. v: line showing strong latency phenotype. vi: weak phenotype and very few neurons labeled.

3.4.2: Participation of the NP4820-labeled neurons in the control of run-to-turn transitions

To examine the potential sensorimotor defect underlying the loss-of-function of NP4820-Gal4, we gathered higher n behavioral data in a slightly modified assay presented in Figure 3.1A. Single larvae were introduced under the odor source. As expected, positive controls (w1118 x UAS-TNTE) display back-and-forth movements under the odor source. After having approached and overshot the source, a run down-gradient is quickly followed by a turn that reorients the larva toward the source (Figure 3.2B, left panel). 20 animals were tested in 2 different odor concentrations for 1-Hexanol (30 mM and 125 mM). Additionally we tested second odor ethyl butyrate, to confirm the effect is not specific to one odor, or one set of neurons activated specific to 1-Hexanol. Depending on the concentration, Ethyl butyrate activates only 1 OSN, while 1-Hexanol activates up to 5 (Kreher, Kwon et al. 2005). Making use of previously established metrics (Gomez-Marin, Stephens et al. 2011), we quantified the phenotype of NP4820>UAS-TNTE for all 4 conditions (Figure 3.2B,C).

Generally, we saw a reduced ability to accumulate under the odor source (Figure 3.2B), as quantified by a decreased odor zone index (Figure 3.2C, upper panels). This effect was depending on the strength of the stimulus, higher odor concentrations partially rescuing the phenotype. More detailed quantification revealed a drastic decrease of cast/turn

events, while run length was increased up to 8 times (Figure 3.2C, middle panels). The runs tended to be straight, as quantified by the persistence (Figure 3.2C, lower panels). This was not due to the mere absence of odor information, as the phenotype was clearly distinct from anosmic larvae lacking the Orco receptor, or wild type larvae foraging in an empty arena without odor cue (Supplementary Figure S1). These animals show an odor zone index close to zero; however, their turning frequency is not much reduced (Figure 3.2B, Supplementary Figure S1C). We concluded that larvae lacking synaptic transmission in NP4820 neurons are impaired in proper timing and/or execution of the cast/turn mode, however still properly perceiving and integrating primary sensory information.

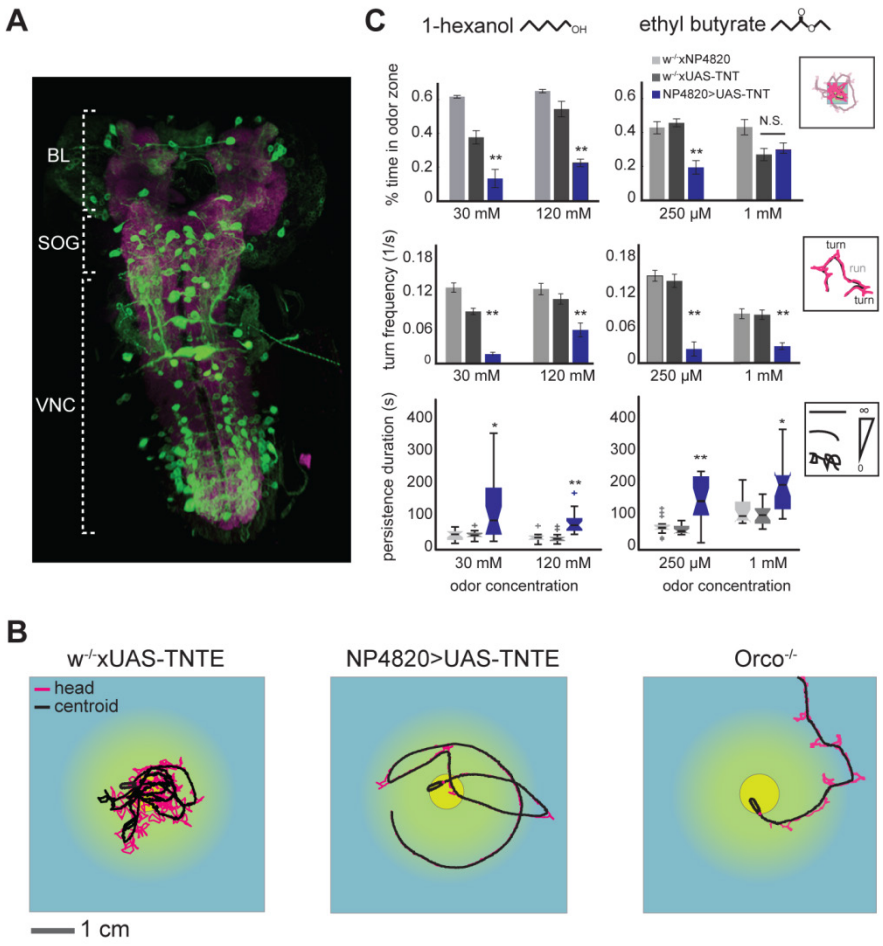

Figure 3.2: Characterization of the anatomy and loss-of-function phenotype of NP4820>UAS-TNTE A: Neurons covered by NP4820-Gal4 line when crossed to UAS-mcd8GFP at the third instar. Green: anti-GFP, magenta: anti-nc82. **B:**The loss-of-function phenotype of NP4820>UAS-TNTE shows an alteration in its orientation behavior compared to positive ($w^{-/-}$x UAS-TNTE, left panel) and anosmic controls ($Orco^{-/-}$, right panel). Each panel represents one illustrative trajectory with the position of the centroid (black) and the head (magenta). Larvae foraged in an odor gradient generated by a single odor source (1-hexanol, 30mM). **C:** Behavioral quantification of the chemotactic behavior of NP4820>UAS-TNTE. The percentage of time in the odor zone and turn frequency are strongly reduced (upper and middle panels); N=18 trials; error bars indicate one SEM; comparisons with both parental controls with a two sample t-test (**p<0.01 upon Bonferroni correction). Persistence length is significantly increased upon loss-of-function (lower panel). In the box plots, the median is indicated by the black vertical line.

Box boundaries represent first and third quartiles; whiskers are 1.5 interquartile range; outliers are indicated by hatch marks.

We then asked if the cast/turn behavior is not only ill-timed, but also altered in its execution. Quantifying the turning in respect to sensory history, we found, that although NP4820-silenced animals turn much less and delayed, they still do turn when experiencing a negative gradient. The larvae thus were still able to detect the slope of the gradient recently experienced. Furthermore, quantifying the probability of turning toward the local odor gradient revealed that the reorientation performance of the mutant is not significantly different from the positive controls (Figure 3.3B). However, the stereotypy of the cast/turn behavior was clearly altered (Figure 3.3C). A wild-type larva typically stops after a 10 second run, immediately casting 1-3 times to either side and engaging into a new run corresponding to the last cast side (Gomez-Marin, Stephens et al. 2011, Lahiri, Shen et al. 2011). Larvae lacking NP4820 neural activity slowed down or stopped for several seconds before reorientation. In several cases, long phases of backing-up were observed, a behavior never seen in wild type. Head casting was slow and less pronounced as in wild type (Figure 3.3B). We found that also head casting performance could be rescued by higher odor intensities, ruling out a mere motor defect, as the animals could in fact execute the behavior under certain conditions.

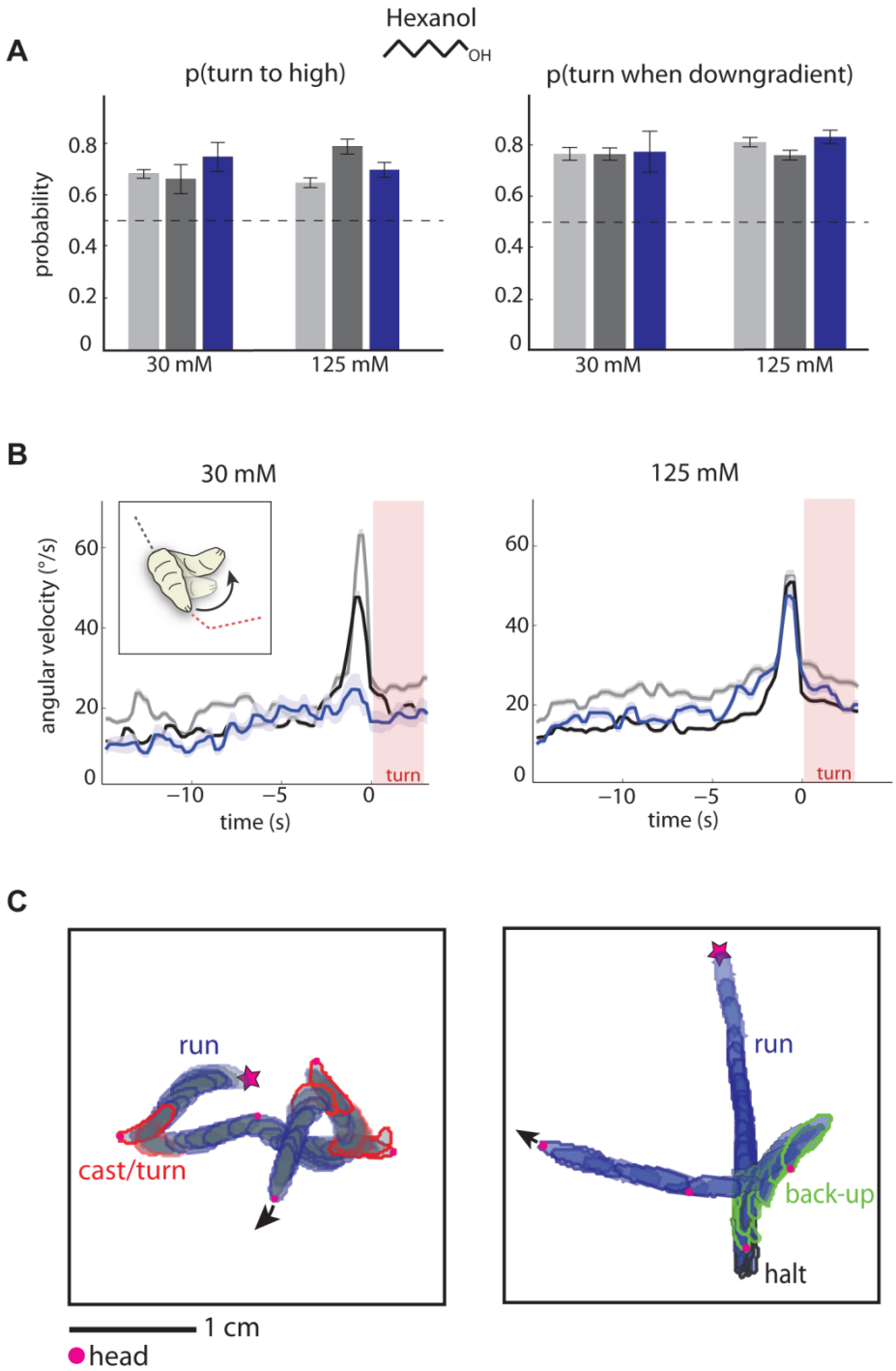

Figure 3.3: High-resolution analysis of the reorientation performances of NP4820>UAS-TNTE A: Temporal sequence of larval postures during chemotaxis.

A posture is represented every 1.5 s. The contour of the larva is color-coded according to the behavioral state: run–blue, halt–black, head cast–red, reversal/back-up– green. At representative time points, the head position is indicated by a small magenta dot. The stereotyped transition from run to cast to turn observed in wild type larvae (left panel) is severely altered in NP4820>UAS-TNTE larvae, which employ halts and reversals instead (right panel). **B:** Detailed analysis of the ability of NP4820>UAS-TNTE larvae to orient toward the odor gradient. Left panel: percentage of turns initiated when the larva is running down the gradient (when-to-turn decision). Right panel: percentage of turns oriented toward the odor gradient (where-to-turn decision). For both metrics and source concentrations, the controls and NP4820>UAS-TNTE are significantly different from chance (dashed line) (Sign test, $p<0.001$). Statistics calculated on N=18+-2 trials. **C:** Analysis of the stereotypy of head casting preceding a turn. Turn-triggered average of the angular head speed for the controls and NP4820>UAS-TNTE according to the color code shown in panel B. At low stimulus concentrations, larvae without functional NP4820-labeled neurons fail to execute stereotypic head casts before turning (left panel). This defect is compensated at high stimulus concentrations (right panel). N=18+-2 trials, shaded area represents 1 SEM.

The expression pattern comprised several neurons in the brain lobes, a group of neurons in the SOG and quite many in the ventral nerve chord including possible glutamergic motor neurons. Given our behavioral results, we wanted to rule out any contribution of motor output neurons. Making use of tsh-Gal80, we could effectively suppress GFP and thus TNT-Expression the neurons located in the VNC (Figure 3.5C). We found that in fact none of the VNC neurons are required for eliciting the phenotype (Figure 3.5A,B).

3.4.3: Sufficiency of NP4820 neurons to induce head casting episodes

To confirm the function of the remaining neurons, we then performed a gain of function experiment, probing the behavioral effect of NP4820 activity. To address this question, we expressed the temperature-gated ion channel dTrpA1 in the NP4820-Gal4 positive neurons (Hamada,

Rosenzweig et al. 2008). The dTrpA1 channel is in the open configuration at temperatures higher than 28 degrees, which induces a tonic firing of the neuron where dTrpA1 is ectopically expressed (Pulver, Pashkovski et al. 2009). We subjected larvae to a temperature ramp ranging 25 and 32 degrees. At temperatures above 25 degrees, the innate response of wild type larvae is a typical escape behavior (Garrity, Goodman et al. 2010). This escape behavior translates into a suppression of turning and an elongation of straight runs (Figure 3.4A, left panel). In contrast, NP4820-Gal4>TNT-E larvae engage in vigorous head casts as soon as the temperature rises above 28 degrees (Figure 3.4A, right panel, supplementary videos M1 & M2). The gain-of-function phenotype was quantified by measuring the average head speed corresponding to 1-degree temperature bins (Figure 3.4B). Since the gain-of-function was preserved in the absence of dTrpA1 expressed in the VNC using tsh-Gal80, we conclude that artificially activating the central neurons labeled by the NP4820-Gal4 line is sufficient to efficiently promote the initiation of a reorientation maneuver starting by an episode of head casts. The fact that larvae tend to arrest in the head casting phase of the reorientation maneuver might be due to persistent activation of the neurons through the effect of dTrpA1.

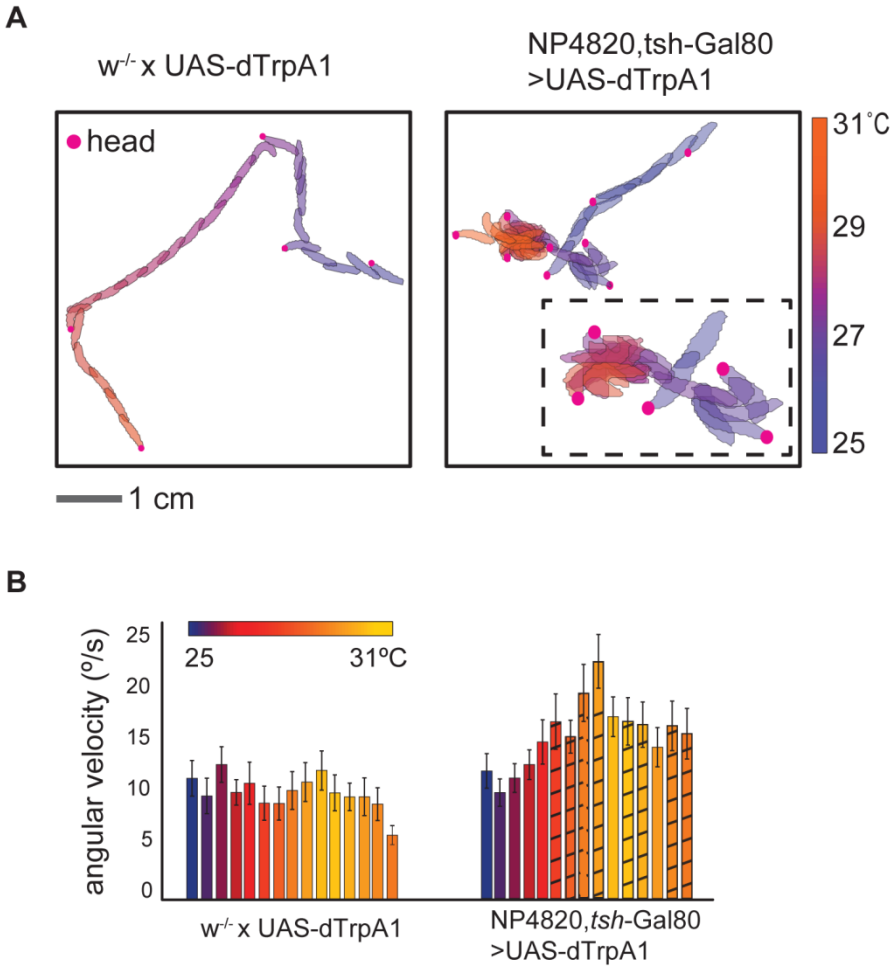

Figure 3.4 Sufficiency of NP4820 neurons to initiate a cast/turn maneuver. A: Rendered neural populations covered by NP4820>*Cha3.3*-Gal80;UAS-mcd8GFP (iv) and NP4820,*tsh*-Ga80>UAS-mcd8GFP (v). Neurons in the SOG are labeled only when using *tsh*-Gal80 but not when using *Cha3.3*-Gal80 are colored in yellow. Neurons common to both driver combinations are colored in blue. **B:** Gain-of-function phenotype: NP4820-positive neurons in SOG plus the brain lobe (BL) elicit head casting when artificially activated. Top panel: trajectory segment illustrating the body postures during a heat ramp ranging from 24 to 31°C (temperature reported by the Peltier sensor). The behaviors of the control $w^{-/-}$ xUAS-dTrpA1 (left) and NP4820-Gal4>UAS-dTrpA1 (right) differ dramatically. The color of the contours corresponds to the temperature of the agar surface on which the animals move freely. Contours are reported every 1.5s. Magenta circles indicate head position. Lower panel: angular velocity of the larva's head (°/s) binned by experienced temperature. Ruled bars indicate bins with a head velocity

significantly higher in NP4820,*tsh*-Gal80 larvae compared to the respective control bin (t-test, N=21 trials, $p<0.05$). Error bars indicates 1 SEM.

3.4.4: Linking of the loss-of-function phenotype to the suboesophageal ganglion (SOG)

Having confirmed both the necessity and the sufficiency for head casting of the NP4820 neurons located in the brain lobes and the SOG, we wanted to further confine the respective population of cells. To this aim we tried to identify the neurotransmitter(s) related to the cells. We tested anti-dopamine, anti-TH, anti 5-HT (serotonin) and anti GABA antibodies. However, despite of assigning glutamine to the putative motor neurons (in fact supporting our hypothesis of their function), and serotonin to 1 cell in the SOG, we couldn't find any neurotransmitter prominently related to the NP4820 cells (data not shown). Another important *Drosophila* neurotransmitter is acetylcholine. ChaT-antibody (raised against choline acetyltransferase) hardly stains the somata of the cells, making it difficult to colocalize it with GFP-labeled neurons. We therefore used an additional Gal80 line: 3.3Cha-Gal80. (Kitamoto 2002). This line comprises 3.3 kb of 5'-flanking DNA of the choline acetyltransferase gene (*Cha*) fused to the GAL80 gene, suppressing transcription of TNTE or mcd8GFP large subsets of cholinergic neurons. Detailed assessment of the remaining neurons showed that the NP4820 neurons in the central brain and several of the ventral nerve cord were not affected. In contrast, the neurons located in the SOG were nearly completely subtracted from the original, leaving just one cell GFP-labeled. We found that for these larvae (NP4820-Gal4> UAS-TNT;3.3Cha-Gal80) the phenotype was completely rescued (Figure 3.5). This intersectional Gal80 analysis therefore allowed us to map the circuit elements underlying the phenotype

to approximately 17 neurons in the SOG and possibly one more neuron located in the basal ganglion (Figure 3.5C,D).

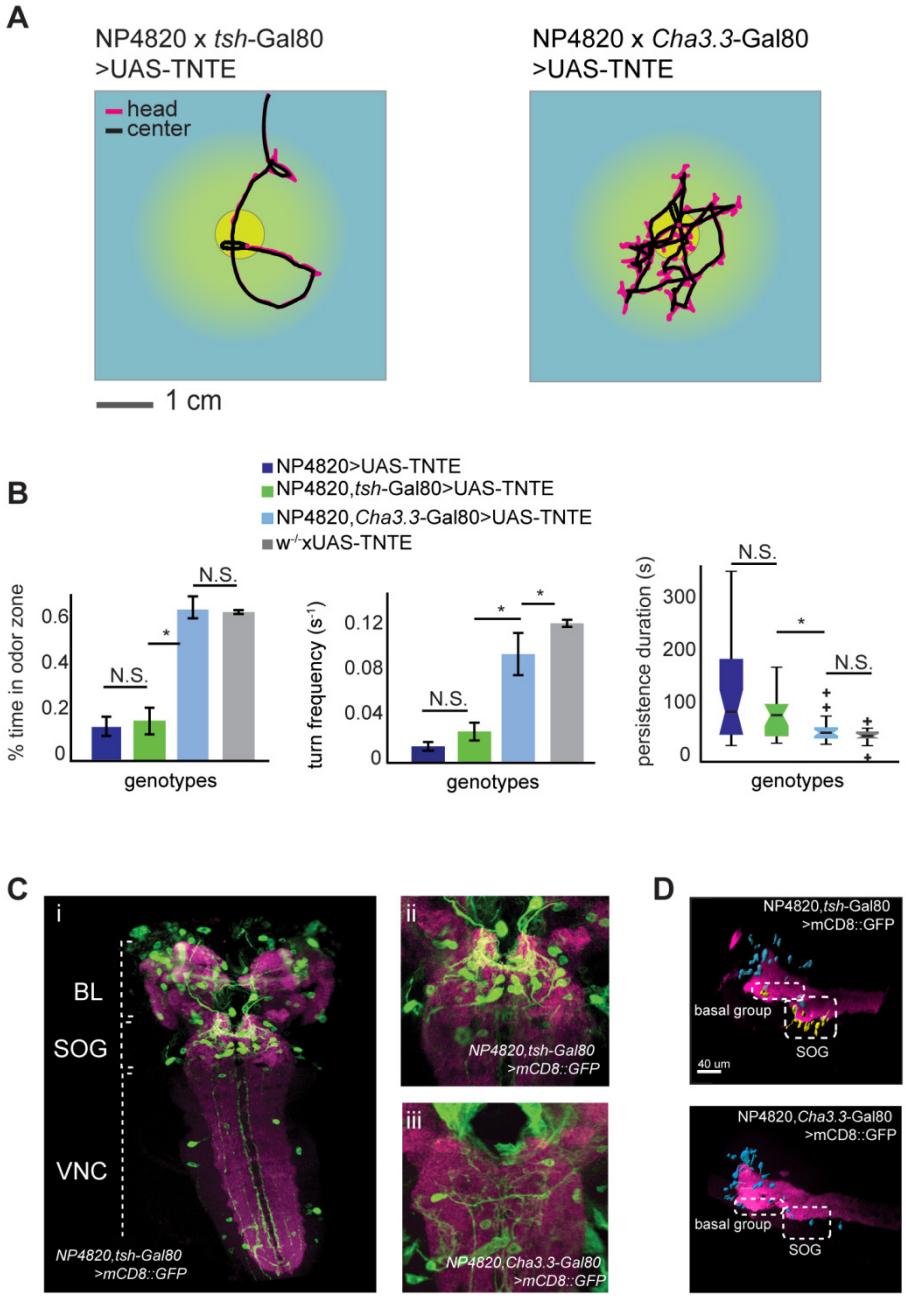

Figure 3.5: NP4820-positive neurons in the SOG are responsible for the phenotype. A: Illustrative trajectories of larvae with two distinct subsets of the NP4820-positive neurons silenced. Left panel: restoration of the VNC function by negative subtraction with *tsh*-Gal80 (NP4820-Gal4,*tsh*-Gal80>UAS-TNTE). In these larvae, the brain lobe (BL) and SOG neurons are still silenced. Right panel: Phenotype is rescued by restoration of the function of cholinergic neurons using *Cha3.3*-Gal80 (NP4820-Gal4>*Cha3.3*-Gal80; UAS-TNT). In these larvae, BL neurons are silenced but the SOG and part of the VNC neurons are functional. **B:** Quantification of chemotaxis behavior after combinatorial silencing of NP4820 subsets. Mean odor zone index, error bar = 1 SEM, n=17+/-3, **p<0,01 via on-way ANOVA, Bonferroni corrected. The turn frequencies (left panel) were undistinguishable between wild type control and NP4820,*Cha3.3*-Gal80>UAS-TNT(light blue) and between NP4820,*tsh*-Gal80>UAS-TNT(green) and NP4820>UAS-TNTE; N=13-19 trajectories; error bars indicate 1 SEM. Comparisons of the mean percentage of time were conducted with a one-way ANOVA followed by a *post-hoc* test based on Bonferroni correction (*p<0.05). The persistence duration (right panel) is increased upon loss-of-function for NP4820,*tsh*-Gal80>UAS-TNT but not for NP4820,*Cha3.3*-Gal80>UAS-TNT; N=13-19 trajectories; error bars indicate 1 SEM. Comparison of the medians were achieved with a Kruskal-Wallis test followed by a *post-hoc* test based on Bonferroni correction (*p<0.05). In the boxplot, the median is indicated by the black vertical line. Box boundaries represent first and third quartiles; whiskers are 1.5 interquartile range; outliers are indicated by hatch marks. **C:** Expression patterns of the combination of driver lines used for restrict the coverage of NP4820 line. Green= anti-mcd8GFP, magenta= anti-nc82. Panel i: Combination of NP4820-Gal4 with *tsh*-Gal80 leads to a nearly complete subtraction of neurons located in the VNC. Panels ii-iii: combination of NP4820 with *Cha3.3*-Gal80 completely abolishes expression of Gal4 in the SOG, except for one neuron. A close-up view of the SOG region is shown for NP4820,*tsh*-Gal80>UAS-mcd8GFP (ii) in comparison with NP4820>*Cha3.3*-Gal80;UAS-mcd8GFP (iii). Green= anti-mcd8GFP, magenta= anti-nc82. **D:** Rendered neural populations covered by NP4820>*Cha3.3*-Gal80;UAS-mcd8GFP (iv) and NP4820,*tsh*-Ga80>UAS-mcd8GFP (v). Neurons in the SOG are labeled only when using *tsh*-Gal80 but not when using *Cha3.3*-Gal80 are colored in yellow. Neurons common to both driver combinations are colored in blue.

By temporally controlling the expression of the TNT effector using a temperature-sensitive isoform of Gal80 (McGuire, Mao et al. 2004) (see experimental procedures), we verified that the phenotype is not due to developmental defects resulting from the silencing of the NP4820-labelled neurons during embryonic stages (Figure 3.6). Together, these observations indicate that the phenotype arises from a loss of function in a circuit located in the SOG upstream of the VNC motor system.

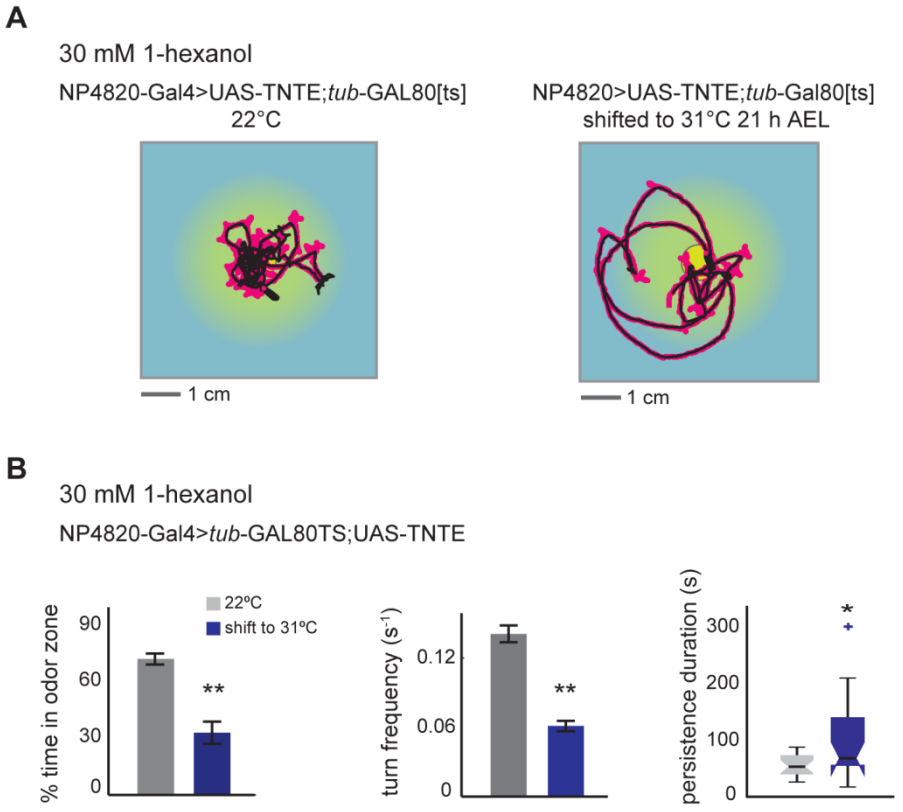

Figure 3.6 Quantification of loss-of-function phenotype after temporal restriction of TNT expression. A: Illustrative trajectory of NP4820>tub-Gal80[ts];UAS-TNTE. Animals tested in a 30 mM 1-hexanol gradient. Control animals raised at 22°C throughout development (left panel). Larvae shifted to 31°C (right panel). We defined the parameters of our experiment based on the results of ref. (Thum, Knapek et al. 2006). Freshly laid eggs developed at 22°C for 19 hours. They were then either kept at 22°C (control) or shifted to a temperature of 31°C until the 5-day-old larvae were collected for behavioral tests in the chemotaxis assay. Single animals were tested one at a time. **B:** Behavioral quantification: when synaptic silencing is achieved by elevation of the temperature to 31°C 21 hours after egg laying, the mean percentage of time spent in the odor zone and turning frequency of the loss-of-function larvae are reduced (left and middle panels, error bars indicate SEM; two-sample t-test; **$p<0.01$ upon Bonferroni correction). The persistence length is increased (right panel). Medians are compared by the Wilcoxon ranksum test (**$p<0.01$). N=17 trajectories.

3.4.5 Generalization of chemotactic phenotype to phototaxis

Finally, we asked whether the NP4820-positive neurons are specific to the sensorimotor pathway underlying chemotaxis or if their function pertains to other types of sensory-driven orientation behaviors as well. To address this question, we examined the phototactic behavior of NP4820>UAS-TNTE larvae. During most of the larval stage, *Drosophila melanogaster* is strongly repulsed by light (Keene and Sprecher 2012). This aversion behavior was elicited by the use of a Gaussian light well — a landscape where the absence of light at the center of an arena represents a zone of comfort (Figure 3.7A). Single larvae were introduced at the point of minimum intensity of the light well. In positive controls ($w^{-/-}$), movement away from the dark center quickly lead to an aversive response that reorients the larva back toward the area of minimum light intensity (Figure 3.7A, left panel). In accordance with the chemotactic phenotype, NP4820>UAS-TNTE larvae took considerably longer before responding to an increase in light intensity (Figure 3.7A, right panel). The amount of time spent by NP4820>UAS-TNTE larvae in the region of low light

intensities is significantly reduced compared to the controls, as was the frequency of turning (Figure 3.7B). Besides lengthening their runs, NP4820 loss-of-function larvae tend to persist in a given direction of motion longer than the controls, without showing any obvious defect in their ability to discriminate up-gradient and down-gradient experiences (Figure 3.7C).

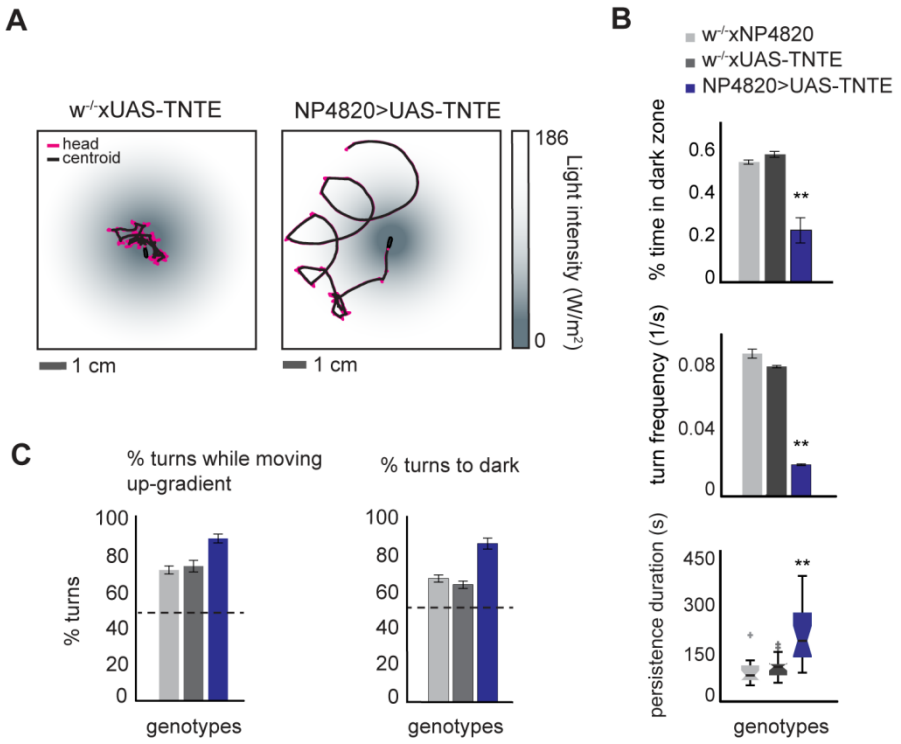

Figure 3.7 Generalization of the function of the NP4820-labeled circuit to the control of phototaxis

A: Illustrative trajectories of photophobic behavior in a light gradient with a Gaussian shape (darkness at the center, full light exposure at the periphery). The control ($w^{-/-}$ x UAS-TNTE) shows strong light aversion, which maintains it at the center of the gradient (left). In contrast, the delayed onset of turns due to the loss-of-function phenotype (NP4820-Gal4>UAS-TNTE) prevents tight accumulation close to the minimum of the gradient (right). In all conditions, the starting position was at the center of the gradient and the larvae were tracked for 5 minutes.

B: Behavioral quantification of the photophobic behavior of NP4820>UAS-TNTE. Percentage of time in dark zone is measured on a 2x2cm area centered on minimum of the light gradient (upper panel). The frequency of turning is strongly

reduced (middle panel) and the persistence duration is increased (lower panel) in NP4820-Gal4>UAS-TNTE larvae compared to control (*p<0.05, **p<0.01, t-test, N=18+-1 trials). **C:** Detailed analysis of the ability of NP4820>UAS-TNTE larvae to orient toward the odor gradient. Left panel: percentage of turns initiated when the larva is foraging up the light gradient. Right panel: percentage of turns oriented away from the light gradient. The results of the controls and NP4820>UAS-TNTE are reported according to the color code shown at the top of panel C. For metrics, the controls and NP4820>UAS-TNTE are significantly different from chance (dashed line), Sign test, p<0.01.

3.5 Discussion

Based on the preliminary data obtained from the primary screen we retested a subset of lines which showed a quantitatively and qualitatively significant phenotype. Our strategy was to both confirm the phenotype and gather more detailed information about the type of behavioral impairment leading to the deficit in chemotaxis, eventually mapping it to one or more behavioral modes underlying taxis behavior. We made use of our custom made tracking software and a refined behavioral assay, testing single animals approaching the odor source in a quantified gradient. We could confirm 75% of the primary hits (i.e. 25% primary screen false positives), which we considered as a positive outcome confirming our quantification strategy applied in the primary screen. The types of phenotypes observed were quite diverse, ranging from inability to initiate normal search foraging, over general locomotor impairment or on the contrary faster and straighter runs. Several lines appeared normal in their locomotion pattern, showing only a strongly reduced chemotaxis performance. When we analyzed the respective anatomical data we observed a correlation of strong phenotypes with relatively high numbers of neurons labeled. The goal of our screen was to assign the behavioral deficit to an amenable number of neurons. We therefore aimed for lines which had a less pronounced phenotype, (i.e. being not completely anosmic) but at the same time covering only a small number of cells, eligible to draw conclusions about their concrete function in sensory-motor-integration. We identified 5 lines accomplishing these constraints. Two of those had to be discarded as the phenotype manifested also in the parental Gal4 line, hinting to the Gal4-element insertion as the primary

cause of the deficit. Finally we decided to focus on the line NP4820, representing the most interesting phenotype in combination with the narrowest expression pattern.

The sensorimotor pathway controlling chemotaxis achieves at least four main tasks: (1) it encodes the stimulus; (2) it integrates dynamical olfactory inputs with other sensory and contextual information, including the internal state; (3) it converts this information into decisions directing the switch between distinct behavioral programs; (4) it implements the execution of specific motor programs. We found that NP4820 covered neurons located in the SOG contribute to the correct switching between behavioral programs. Their silencing causes the larvae to stay extraordinarily long in run mode, increasing run lengths by several 100%. Besides not being timely initiated, also the execution of reorientation maneuvers is altered, being preceded by pause episodes and employing behavioral modes rarely used by a wild type larvae- such as backing up. We conclude that the SOG is part of a circuit element that controls the timing and coordination of reorientation maneuvers.

In fact, constitutive activation of this circuit is sufficient to initiate reorientation maneuvers even in the absence of a gradient. Given that the loss-of-function phenotype affects odor-driven and light-driven behaviors in a similar manner we could rule out the limitation of NP4820 neurons to olfactory processing. At the same time we could dissociate the phenotype from the motor system recently shown to be contained within VNC (Berni, Pulver et al. 2012), an observation that makes a purely motor function very unlikely. Even though we cannot exclude any direct modulatory effect that the identified neurons could exert on the antennal

lobe and the optic neuropil (Sprecher, Cardona et al. 2011, Thum, Leisibach et al. 2011, Das, Gupta et al. 2013), such a mechanism would not explain the induction of head casting upon gain of function. We favor the idea that the identified group of neurons acts on the sensorimotor pathway downstream of the peripheral visual and olfactory and maybe even further systems. Our intersectional strategy led us to the conclusion that a group of cells located in the suboesophageal ganglion (SOG) are underlying the phenotype. However, it is noteworthy that the anatomical assessment remains qualitative and that variability at times hampers completely unambiguous annotation of a specific cell identity in a given specimen. We therefore cannot definitely exclude the contribution of other neuron(s) in the brain lobes.

The SOG - besides being a relay center for taste - may as well constitute a site where contextual information about the sensory environment is combined to direct locomotion through action selection or motor commands. This model is supported by the persistence of the phenotype in the absence of sensory stimulation. Moreover, it is also compatible with the reported function of the SOG in the adult fly (Zhou, Rao et al. 2008), as well as in other invertebrates. For example the medicinal leech where it controls the switch from swimming to crawling (Friesen and Kristan 2007). Together, the results of this study suggest that the SOG acts as a control circuit directing behavior based on changes in the stimulus that are partly induced by the larva's own motion . We propose that the SOG participates in the transformation of multimodal sensory signals into the selection of behavioral routines (straight runs and reorientation maneuvers). Thirty years after the first analysis of larval foraging behavior as a handle on the transition between elementary motor

programs (ethogram) (Green, Burnet et al. 1983), this work represents one of the first attempts to map the neural substrate of decision-making circuits in the *Drosophila* larva. In the future, a combination of optogenetics and functional imaging (Yao, Macara et al. 2012) should help us clarify the mechanisms through which the SOG contributes to the control of orientation.

3.6 Supplementary Information

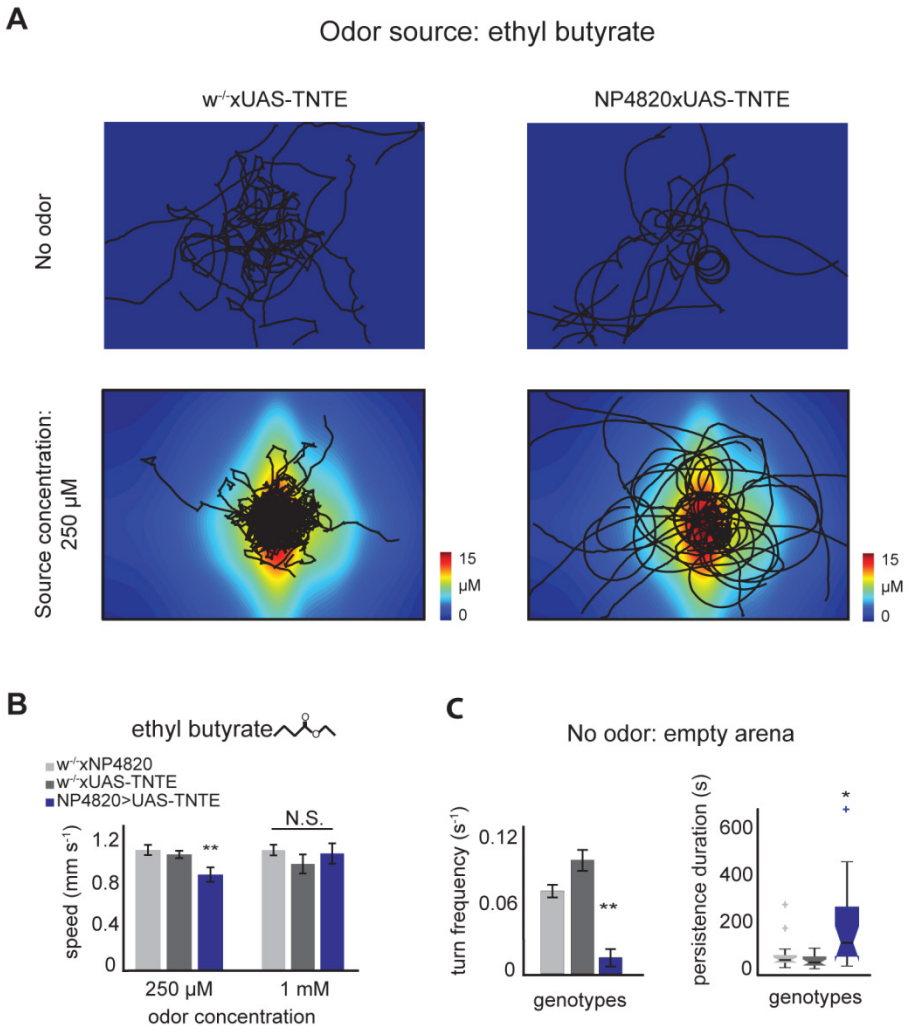

Supplementary Figure S1: Behavior of NP4820>UAS-TNTE and controls in empty arena and reconstructed odor gradients **A:** Plots of superimposed trajectories observed in an arena devoid of odor (upper panels) and a gradient of ethyl butyrate (source concentrations: 250 µM). Left column: wild type control behavior ($w^{-/-}$ x UAS-TNTE). Right column: loss-of-function phenotype of NP4820 (NP4820>UAS-TNTE). For all conditions, 15 to 20 trajectories are shown. The ethyl butyrate gradient at source concentration 250 µM was inferred by scaling the concentration of the reconstructed gradient of panel A by a factor 120. Odor concentration in gaseous phase indicated on the color bar. **B:** Mean

locomotion speed is slightly lower in larvae with silenced NP4820 neurons than in control lines when tested with a low concentration source of ethyl butyrate. This defect is rescued by higher odor concentrations (two-sample t-test, **p<0,01; N=18-20 trajectories; error bars indicate 1 SEM). **C:** Behavior of controls and NP4820>UAS-TNTE in an arena devoid of an odor source. Mean turning frequency is reduced in NP4820>UAS-TNTE compared to the control (left panel); N=15-19 trajectories; error bars indicate 1 SEM; comparisons with both parental controls were carried out by means of a two-sample t-test (**p<0.01 upon Bonferroni correction). Persistence duration is increased upon loss-of-function (right panel). Comparisons with both parental controls were carried out by means of a Wilcoxon ranksum test (*p<0.05 upon Bonferroni correction). In the boxplot, the median is indicated by the black vertical line. Box boundaries represent first and third quartiles; whiskers are 1.5 interquartile range; outliers are indicated by hatch marks.

Supplementary Movies M1 and M2: Locomotor behavior during gain-of-function experiments.
As detailed in the Experimental Procedures, single larvae were monitored while experiencing a temperature ramp from 24 to 31°C. Representative response of a control larva ($w^{-/-}$xUAS-TrpA1, M1) and a larva expressing dTrpA1 in the NP4820-positive neurons (after *tsh*-Gal80 subtraction, M2). In the movie, the appearance of the grey bar on the bottom right corner indicates the time point at which the temperature threshold (28°C) of the dTrpA1 channel is passed and constitutive activity is induced. The movies run at 2x real time.

Chapter 4:

A neural substrate underlying electrotaxis: NP2729-Gal4

4.1 Abstract

Drosophila melanogaster larvae detect and respond to a multitude of sensory stimuli such as temperature, chemicals, light, nutrients and noxious agents. Here we describe a novel sensory modality in the larva: electrosensation. When exposed to a uniform electric field, larvae robustly migrate to the cathode (electron source). This behavior does not depend on a current or an ionic environment. Moreover, larvae quickly respond to changes of field orientation, initiating a cast/turn maneuver to realign themself with the field direction. In a large behavioral screen we identified a neural population underlying the detection of electric fields. Sensory neurons covered by the Gal4 line NP2729 were strongly activated when facing the anode of an electric field. Orientations towards the cathode caused inhibition, suggesting that larvae avoided activation of these neurons by navigating towards the cathode. We found that the response was both tuned to field orientation and strength, covering a range of 0.1 to 5 V/cm. Interestingly, the neurons projected to the suboesophageal ganglion, which we related previously to run maintenance and cast initiation.

To identify the molecular mechanism responsible for neural activation by electric fields we screened several receptor mutants, revealing trp and trpl- members of the transient receptor potential protein family- to be involved in electrotactic orientation behavior. Taken together our result show that electric fields elicit robust behavioral and neural responses in *Drosophila* larvae, corrobating the significance of this sensory modality in invertebrates as well as vertebrates.

4.2 Introduction:

Constant electric fields surround electrically charged particles (Figure 4.1A). The exploitation of electrical signals as a cue within the environment of plants, animals and humans has been known for two centuries. Its effects on living tissue was studied already in 18th century by Luigi Galvani who famously discovered by accident that the muscles of dead frogs legs twitched when jolting them with a spark from an electrostatic machine (Galvani 1791). Electric fields (EFs) also arise naturally in tissues where directional ion transport across intact epithelia causes potential difference directed across the epithelial layer (Figure 4.1B). This field has various implications: It was shown that a variety of cell types (e.g. epithelial cells and neurons) migrate towards the cathode in an uniform EF and that the direction of a field in polarized tissue is used as a cue for cell migration and neural growth cone orientation throughout development (Robinson 1985). Injuries destroy the physical and electrical integrity of epithelia, leading to a change of field direction. This new field was shown to be crucial for wound healing in various species, guiding the migration of neurons and epithelial cells towards the wound opening (Ingvar 1920, McCaig, Song et al. 2009).

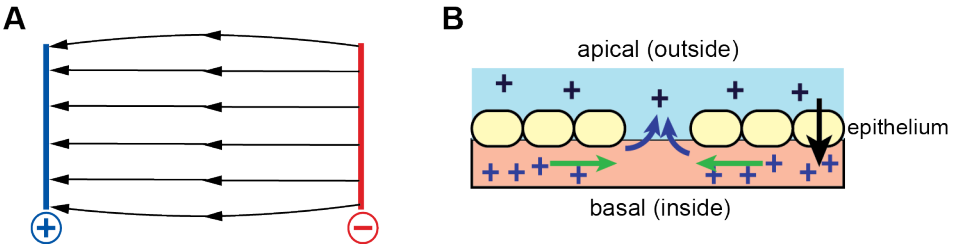

Figure 4.1: Examples of electric fields A: Electric field lines between two linear charges with a constant potential, resulting in a uniform field as used in the electrotaxis assay. **B:** Electric field arising naturally in tissues. Ion channels of epithelial cells establish a potential through the membrane (black arrow). Upon wounding this equilibrium is damaged, cations leak to the apical side and a field specific to the wound establishes (green arrows).

At the macroscopic level, various species detect and navigate in electric fields, having developed specified electrosensory organs to detect a field's orientation and its origin which can be inanimate objects or living organisms such as prey and conspecifics. One prominent example are the ampullae of Lorenzini of cartilaginous fish which serve to sense electric fields in the water (Wueringer 2012). Furthermore, the global atmospheric electrical circuit causes an electric field between the earth, which is negatively charged, and the net positive charge in the air, resulting in a potential difference at the earth's surface of 100 to 300V/m (Siingh D 2006). This field can be detected and exploited by animals to orient.

Recently, invertebrate electrosensation was described for various species. Newland et al revealed that cockroaches avoid static electric fields around 10V/cm in a Y-tube assay, making use of their antennae to detect the field (Newland, Hunt et al. 2008). Electric fields were found to cause a deflection of the antennae and when the antennae were surgically ablated, the ability of cockroaches to evade electric fields was abolished. Clarke et al (2013) report floral electric fields as a cue for bumblebees involved in improving learning and discriminating rewarding resources. Floral electric fields exhibit variations in pattern and structure, which can be discriminated by bumblebees and associated with nectar rewards (Clarke, Whitney et al. 2013). Similarly, Greggers et al (Greggers, Koch

et al. 2013) found that bees emit and detect electric fields, identifying mechanoreceptors in both joints of the antennae as sensors. They documented the presence of axons in the Johnston's organ that are responsive to EFs and suggest their role in social communication. Gabel and colleagues (2007) documented electrotactic behavior in the nematode *C. elegans*. Their comprehensive study reported robust migration of the worms towards the cathode in a uniform field. They provide evidence that the field is detected via amphid sensory neurons located in the head of the worm (Gabel, Gabel et al. 2007) .

Exposing third instar *Drosophila melanogaster* larvae to a uniform electric field, we found that like other species they are robustly navigating towards the cathode. In order to identify neurons underlying this behavior, we included an electrotaxis behavioral assay in the behavioral screen described in chapter 1. A primary screen resulted in more than 40 lines altered in their electrotactic performance. As this behavior was never described before in *D. melanogaster* - neither for the larval nor for the adult stage-detailed metrics defining the orientation strategy remained to be defined. To this aim we performed a detailed analysis of the behavioral paradigms underlying wild type larval electrotaxis using a high-resolution behavioral assay. To further define the nature of the electrotactic defect and the respective neurons of the lines identified in our screen, we decided to first reconfirm the phenotype found in the primary screen repeating the mass assay. Subsequently, we used high-resolution behavioral assay to identify changes in the navigational strategy compared to wild type larvae. Making use of immunolabelling and functional imaging of neural activity, we identified neurons responsible for detecting electric fields. We characterized how these neurons

represent the strength and orientation of the electric field with respect to the larva, and how this information guides orientation responses.

4.3 Material and Methods

Fly stocks and histology: For functional imaging we crossed Gal 4 driver lines to a UAS-GCamp3 (Tian, Hires et al. 2009)triple copy line. Receptor mutants: $cry^{-/-}$(Charlotte Förster, Biozentrum Würzburg), $TrpA1^{-/-}$ (Bloomington #26504), $Nan^{-/-}$ (Bloomington #24902), trpl[MB03075] (Bloomington #23512), trp[MB03672] (Bloomington #23636) Further fly stocks and histology: see chapter 2

Electrotaxis Assay:

Device design details see chapter 2. The behavior was monitored using an adapted computer-vision algorithm previously described (see chapter 2). We used a custom Matlab software controlling both camera acquisition and tracking as well as and voltage level and polarity applied to the platinum wires of the behavioral chamber. Both were synchronized to relate the observed behavior to electric field conditions. Third instar larvae were harvested from the food in 15% sucrose immediately before testing.

Mass assay: A group of ca. 10 third instar larvae were cleaned in dH_20 and placed in the middle of the agarose slab. Animals moved freely for 2 minutes in a 2 V/cm electric field. Pictures were taken every 2 seconds and mean approach to the cathode calculated.

High-resolution assay: Single third instar larvae were introduced in the center of the agarose slab. A static electric of a specific strength was

applied for 30 seconds allowing the animal to align and forage towards the cathode before switching field polarity by 180 degrees. This sequence was repeated 4 times, resulting in a total experimental time of 4 minutes. All behavioral analysis was performed with custom Matlab scripts.

Gain of function-assay: see chapter 2

Functional Imaging: On a standard glass microscope slide (26 x 76 mm, Menzel) 4 platinum wires were mounted in parallel with the slide edges in grooves, fixed and isolated by Epoxy adhesive (Loctite)(fig 12C). The platinum wires were connected to a PC via an analog output device (National Instrument, USB 6009) which to control the voltage applied to each wire separately. Voltage and microscope acquisition was controlled and synchronized via custom Matlab software. Whole or semi-intact larvae (head only) where mounted in the center of the wires in a specific orientation with respect to polarization of the applied field. A minute amount of dental glue applied to the dorsal cuticle was used to immobilize the specimen. The preparation was immersed in deionized water when intact or in a physiological saline previously described for imaging when semi-intact (Asahina, Louis et al. 2009) also connecting the wires and finally covered with a glass cover slip.

Imaging microscope: Leica SP5, sampling at 3.6 Hz

Fluorescence analysis was conducted with Matlab. Each recording was analyzed with a custom-made software. Changes of fluorescence intensity were generally reported as time series of $\Delta F/F = (F-F_0)/F_0$, where F is the raw fluorescence signal and F_0 is the mean fluorescence averaged over 5 seconds before the onset of the stimulus. For unbiased detection of regions of interest responding to the field stimulus image data were filtered and down sampled before correlating the $\Delta F/F$ signal of each

pixel with the voltage stimulus applied. Pixels strongly correlated (activation) or anti-correlated (inhibition) resulting in a significant correlation (i.e. a correlation coefficient larger than 0.35 or smaller than -0.35 respectively) where identified. The alpha value corresponding to the correlation cutoff value was chosen based on qualitatively validating results on several preps. $\Delta F/F$ values for the specific neurons were then obtained by calculating intensity time course in a region of interest selected manually based on the correlation analysis.

Behavioral Quantification

Mass assay: mean distance from the cathode was calculated as described in Chapter 2. We then calculated the mean approach to the cathode as the mean percentage of total distance travelled from the starting point to the cathode.

Single animal analysis: heading was calculated as the instantaneous angle of the centroid relative to the electric field at 1Hz. Absolute bearing was calculated as the absolute deviation of heading angle relative to the field direction. For all angular data circular statistics were applied.

4.4 Results

4.4.1 Electrotaxis behavior in *Drosophila melanogaster* larvae

To gather more detailed insight in larval electrotactic navigation, we assessed the behavior both in a mass assay and a high-resolution assay for single animals. Larval electrotaxis is a robust behavior, leading to navigation towards the cathode when animals are exposed to uniform electric field (Figure 4.2A). The sensory threshold as defined by a significant mean approach to the cathode compared to no field conditions (Figure 4.2B) was around 0.17 V/cm. We observed electrotaxis in a range of field strengths up to 4 V/ cm, however, fields higher than 6V/cm lead to nearly complete paralysis. Electrically induced paralysis was reversible; larvae almost immediately resume crawling after switching off the field or reducing its strength. Interestingly, the range of electric field strengths evoking taxis was within the order of magnitude detected by C. *elegans* (3-14 V/cm) and the bumblebee *Bombus terrestris* (20V/cm) (Gabel, Gabel et al. 2007, Clarke, Whitney et al. 2013).

Since the crawling substrate was devoid of ions no or only minute currents below the detection threshold of our setup (2mA) were induced. We conclude therefore that the electric field itself is directing the motion. However, the larva and its cuticle surface is not devoid of ions, local currents created by ions stemming from the animal itself could possibly contribute to the detection of the field. In fact, electrotaxis is not impaired in an ionic environment, as animals equally approach the cathode on an agarose arena containing 100 mM NaCl (Figure 4.2C). Making use of a high-resolution tracking algorithm (Gomez-Marin, Stephens et al. 2011), we quantified the behavior of single animals in the electric field. Larvae

were introduced at the center of the agarose arena and an electric field of 2V/cm was applied. After 30 seconds, the field direction was inverted, probing the ability of larvae to make a U-turn and realign to the new field direction. For each animal the sequence of field swaps was repeated 4 times. We found that the mean heading angle of wild type animals is close to perfect alignment with the direction of the field (Figure 4.2D). However, the variance of the bearing angle is quite large, on average the animals absolute heading angle relative to the direction of the field (bearing angle) is around 50 degrees (Figure 4.2E, left panel). Mean bearing stays constant when the animal is exposed to one field direction (Figure 4.2F). Swapping field direction by 180° reliably induces head casting and a turn which quickly realigns the animal to the new field direction (Figure 4.2 E,G). During constant field conditions, turns are induced after an episode of large absolute bearing indicating an unfavorable heading of the animal and turns improve orientation by realigning towards the direction of the cathode, reducing the bearing angle. Interestingly, bearing history before turns do not show a stereotypic sharp transition from good alignment to worse alignment as seen in chemotaxis (Gomez-Marin, Stephens et al. 2011). In fact, absolute bearing angle already declines preceding the turn, suggesting that the larva corrects its alignment while still in a run. Moreover, mean bearing never exceeds 90 degrees, showing that foraging opposite to the field direction is effectively avoided by the larva, both by means of turning and run direction.

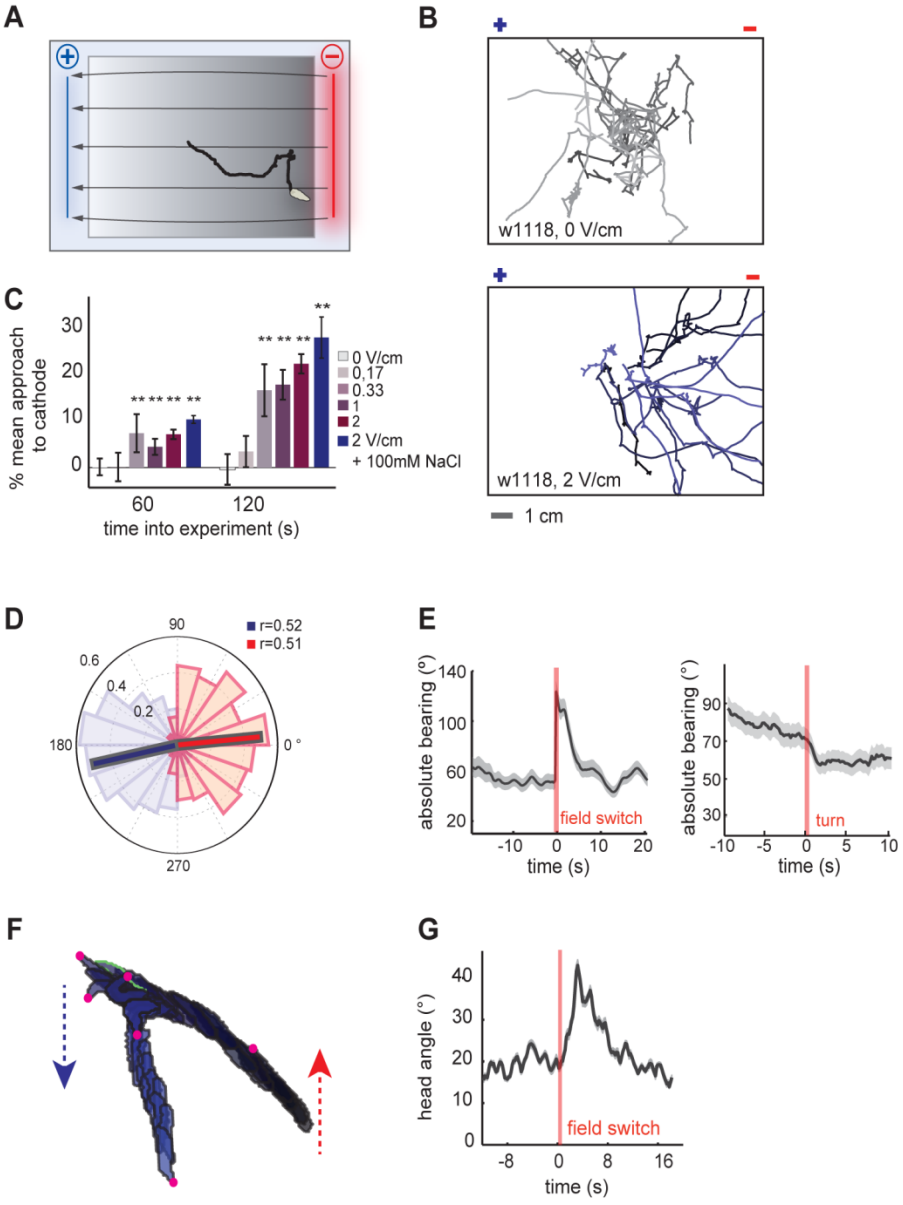

Figure 4.2 Larval behavior in a uniform electric field A: Schema of the electrotaxis behavioral assay. Typical behavior is illustrated by a wild type trajectory (black line). The Larva was introduced in the middle and foraged to the cathode. **B:** Overlay of 15 trajectories of single wild type larvae foraging for 3 minutes in the electrotaxis arena. Upper panel: no electric field, lower panel: electric field =2V/cm**. C:** Mean approach to the cathode in an electrotaxis mass

assay in deionized water and agarose or with 100 mM NaCl added, n=4 trials**. D:** Normalized polar histogram of heading angles of single larvae exposed to 180-degree switches in the direction of the electric field. Grey framed bars indicate mean heading angle, for the respective field direction. N=18 animals, 8 field switches each**. E:** Mean absolute bearing angle before and after a switch (left panel) and before turns executed during constant field conditions (right panel). Red bar indicates time point of field switch or turn onset, respectively. N= 18 animals, grey shaded area indicates 1 SEM**. F:** Trajectory segment illustrating the head casting episode triggered by a field switch. Larval body postures are depicted at 1,5 Hz. Head positions are marked by magenta dots, the green contour indicates time point of field switch. Field direction is indicated by arrows (red: before switch, blue after switch). **G:** Head casting quantification. Mean head angle before and after field switch, N=18 animals, shaded area indicates 1 SEM.

4.4.2 Secondary Electrotaxis Screen.

We re-screened 43 Gal4 lines which showed an electrotaxis phenotype in the primary screen, excluding lines with a pronounced locomotion deficit. After crossing them to UAS-TNTE and testing them in the same electrotaxis mass assay as used in the primary screen, performing at least 3 more runs, we could confirm the behavioral deficit for 15 lines. Discarding also additional 6 lines with a milder locomotion phenotype, we continued assessing the neurons labeled by the respective drivers performing immunolabelling on 9 final Gal4 lines by crossing them to UAS-mcd8GFP. 3 lines did not produce offspring; hence we finally obtained results for 5 lines (table 2).

Gal4 line	expression pattern
NP1288	only mushroom body
NP1323	busy
NP2729	trachea, very sparse
NP3078	medium sparse
NP7374	very busy

Table 2: NP Gal4-lines with a reproducible deficit in electrotactic behavior when driving TNT expression.

Within this group of fly lines we found the line NP2729-Gal4, showing a persistent strong phenotype, resulting in a nearly random distribution of the larvae in the electric field (Figure 4.3A). At the same time an exceptionally low number of neurons were labeled (Figure 4.3B). It showed strong GFP expression throughout the tracheal system, however only 5 central neurons were labeled. Interestingly, we also found expression in 4-6 peripheral neurons located in the terminal and the dorsal organ of the larva (Figure 3A). Given the strong phenotype and the small neuron number affected, we focused our analysis on this line. We found that the alignment to the field of NP2729>UAS-TNTE was severely hampered compared to wild type (Figure 4.3C). Although the movement towards the cathode was not fully abolished, the overall performance was significantly worse, including single animals which appeared to not detect the field at all. Alike the impaired alignment to the static field, the detection of field changes was strongly diminished. The stereotypic head cast following a field swap was less pronounced and realignment to the new field direction slower and imprecise (Figure 4.3 E,F) . The Gal4 insertion was located in the gene Ataxin-2 binding protein 1 (*dA2BP1,* CG32062*)* known to be involved in neural function in mammals including human. Expansion of polyglutamine repeats in Ataxin-2 causes spinocerebellar ataxia type 2 (SCA2), a neuro-degenerative disease. Ataxin-2 binding protein modulates its activity by binding to the C-terminus (Usha and Shashidhara 2010). In *D. melanogaster* it was shown to be required for the development of the embryonic nervous system and wing vein patterning. It was also found in a screen for genes expressed in

the olfactory organs of the adult fly, mutants showing a reduced responses to benzaldehyde (Tunstall, Herr et al. 2012). We therefore wondered if the P[Gal4] insertion itself could interfere with neural function causing a behavioral deficit. Equally, the expression of tetanus toxin in the tracheal system could be the origin of the behavioral effect. In order to rule out any contribution other than neural function we applied an intersectional strategy using the NP2729 driver line in combination with Cha3.3-Gal80 and UAS-TNTE which suppressed toxin expression in all neurons covered by the driver line, leaving only trachea labeled. Applying the same assay and quantification as for NP2729>UAS-TNT, we could not detect any behavioral impairment for this genotype. Therefore, we concluded that either the peripheral or the central neurons where responsible for the phenotype.

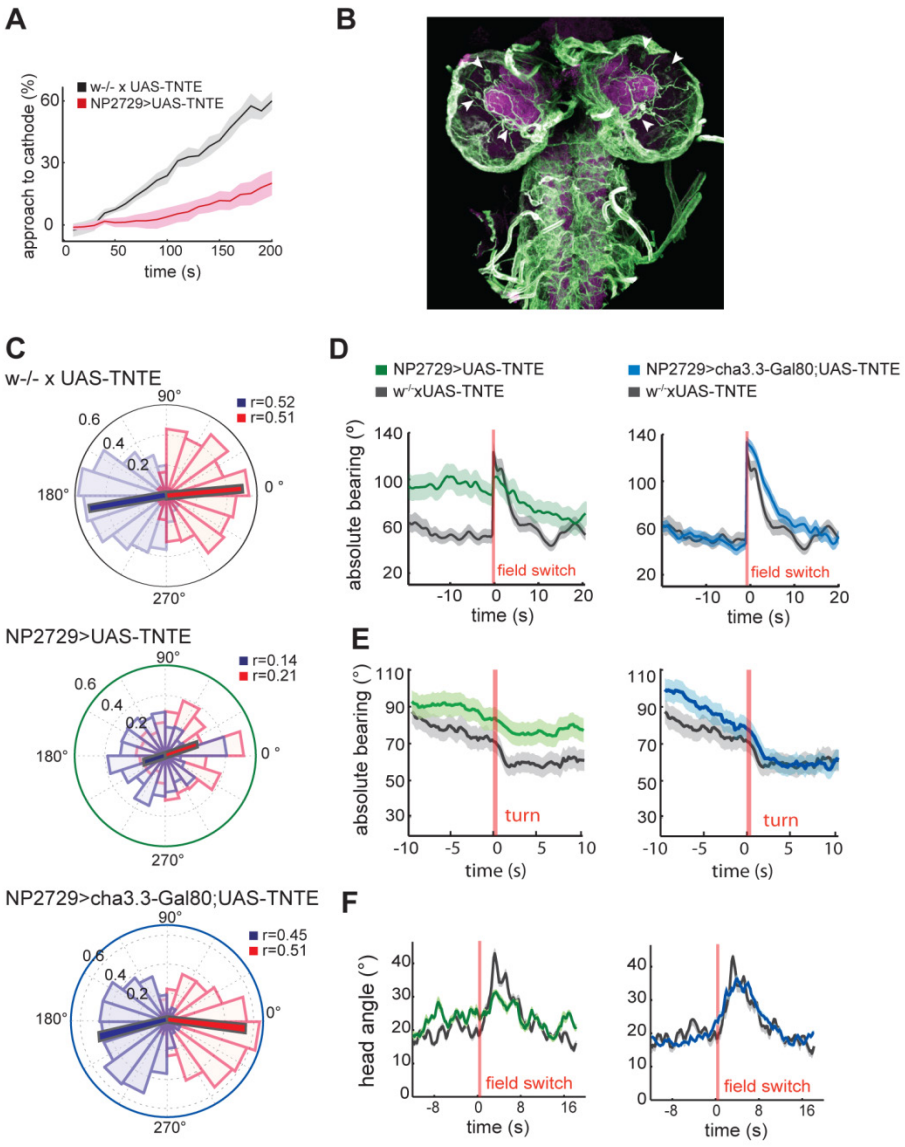

Figure 4.3: NP2729 silences neurons essential for electrotaxis. A: Mean approach to the cathode in a mass assay. Black: wild type control, red: NP2729-Gal4 driving TNTE expression. Shaded area represents 1 SEM. **B:** Immunolabeled third instar larval brain showing expression pattern of NP2729-Gal4 driving UAS-mcd8GFP, green: anti-GFP, magenta: anti-nc82 (neuropil), arrow heads indicate position of central neuron somata. **C:** Heading angle polar plot and circular mean. Upper plot: wild type control, middle plot: NP2729>UAS-TNTE, bottom plot: NP2729>cha3.3-Gal80;UAS-TNTE. Grey framed bars indicate mean heading angle for the respective field direction, circular variance r is indicated in the

legend. N=18+-1 animals. Mean heading was significantly different from wild type (Watson and William's test, $p<0.01$) **D:** Mean absolute bearing before and after a field switch. N=18 animals, shaded area indicates 1 SEM. **E:** Mean absolute bearing history prior and after turns during constant fields. Black: wild type. N=18+-1 animals, wt: 151 turns, NP2729>cha3.3Gal80;UAS-TNTE:172 turns,. **F:** Mean switch-triggered head angle. Shaded areas represent 1 SEM, n=18+-1 animals

4.4.3 Sensory neurons responsive to electric fields

Based on our behavioral findings, we hypothesized that the peripheral neurons located mainly in the terminal organ of the larva (Figure 4.4A) could contribute to the detection of electric fields. The Gal4 line covered 5 neurons in the terminal organ ganglion and 3 neurons on the dorsal organ ganglion. To investigate the neural activity of these neurons in response to electric fields, we developed a preparation for functional imaging of the neural response of the respective neurons expressing a genetically encoded calcium indicator (GCamp) under the control of NP2729-Gal4. The GCamp family of calcium indicators is composed of a single circularly permuted GFP linked to calmodulin and its binding peptide myosin light-chain kinase M13. Upon calcium binding, conformational changes in the Calmodulin/M13 complex cause a fluorescence change in the circularly permuted GFP-based fluorophore (Akerboom, Rivera et al. 2009) . The changes in fluorescence level can be used as a proxy for neural activity, leading to Ca^{++} influx at the synapse.

Applying electrical fields within the range of robust behavioral responses we could detect a strong response in a subset of the 8 peripheral neurons. We first mimicked the conditions in the behavioral arena swapping the field direction by 180 °, the anterior-posterior body axis corresponding to 0 degree. In every tested animal at least one neuron was

strongly activated by a negative field aligned to the neurons axis. A 180° change of field direction caused an inhibition of the same neuron. In several animals we also found neurons which appeared to be only inhibited by the positive field. Fields oriented perpendicular to the animal axis didn't cause a significant response (Figure 4 E), irrespectively of the field orientation (90° or 270°).

In order to examine the neural representation of field direction in more detail we tested the response to fields continuously changing it clockwise around the animal's axis. In agreement with the previous regime, we found peak activity to negative fields aligned to the neural axis and inhibition to fields in opposite direction. In addition we found the calcium sensor response generally scaled to the direction of the field relative to the animal. As the total field strength was constant throughout the experiment, we concluded that the alignment to the field itself is captured in neural activity (Figure 4.4E).

Finally we tested the response to graded field strengths, exposing the larvae to ramps of an increasing and decreasing unidirectional negative electric field aligned to the animal. The amplitude of neural response was tightly scaled to the field strength (Figure 4.3G). Onset of a response larger than 10% $\Delta F/F$ was detected at 0.19 V/cm. This was consistent with the sensory threshold established during behavioral experiments.

Next, we aimed at locating the area of central projections of the NP2729 electrosensory neurons. The driver line labeled not only neurons but also the tracheal system whose tubular system appears abundantly throughout the CNS. Therefore we combined btl-Gal80 with NP2729-

Gal4 driving mcd8GFP expression. This impaired GFP expression in the tracheal system and allowed the identification of neural processes. We found two nerves entering the central brain: one targeted the posterior part of the SOG (Figure 4.3B). Notably also the gustatory neurons which reside mostly in the TO, arborize in this region (Colomb, Grillenzoni et al. 2007). The second entered the brain more anterior and projected with little ramification immediately adjacent to the antennal lobe, which itself was devoid of neural arbors (Figure 4.3B). A projection pattern similar to that observed for the Gr2a positive neurons in the DO (Colomb, Grillenzoni et al. 2007).

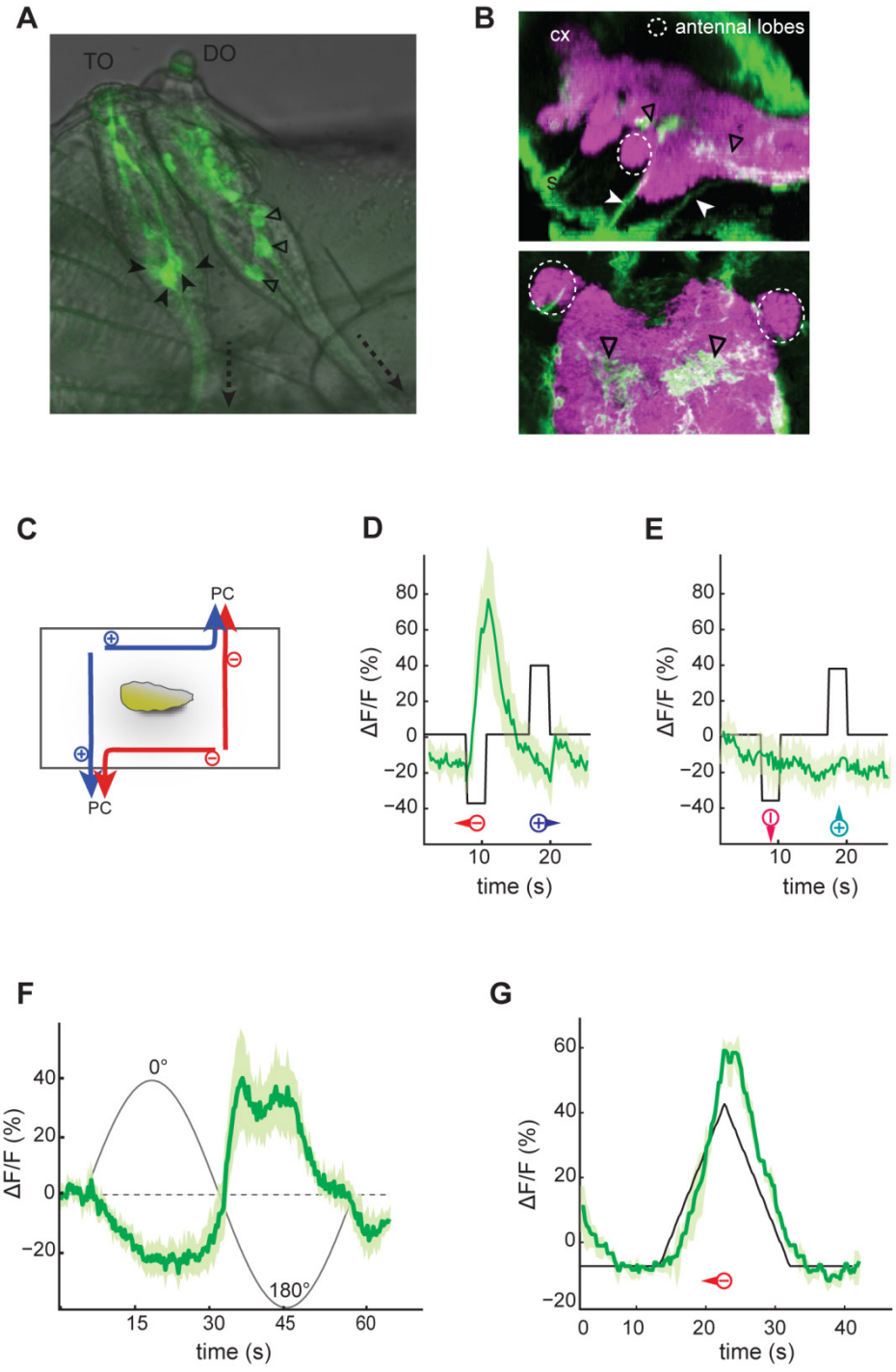
A
TO
DO
B
cx
antennal lobes
C
PC
PC
D
ΔF/F (%)
time (s)
E
ΔF/F (%)
time (s)
F
0°
180°
ΔF/F (%)
time (s)
G
ΔF/F (%)
time (s)

Figure 4.4: Neural encoding of electric fields. A: peripheral neurons covered by the NP2729 Gal4 line, drive expression of mcd8::GFP. Filled arrowheads: neuron somata located in the TO, open arrowheads: neural somata located in the DO. **B:** Central projections of NP2729 labeled peripheral neurons in a third instar larval brain. Green: mcd8GFP, magenta: nc82. Upper panel: lateral projection of the right hemisphere, White arrowheads: nerves labeled by NP2729 entering the SOG, black arrowheads: arborization-fields of the axons of the 2 nerves, , cx=mushroom body calyx, s= neuron somatum. Lower panel: dorsal projection showing arborization of the TO and DO neurons in the SOG **C:** Schematic representation of the imaging chamber used for recording calcium influx upon application of electric fields. Red and blue indicate polarization of the platinum wires. **D-F:** Calcium transients in response to electrical field stimulation. Green: mean ΔF/F (change in fluorescence intensity normalized by baseline fluorescence intensity) from 4 representative preparations, light green indicates 1 SEM. Black: illustrating electric field stimulus(x-scale doesn't apply). **D:** Response to discrete field pulses aligned to the animal. 3 seconds pulses of 2=V/cm were intermitted by 7 second lag phases of V=0. The field was oriented as indicated by the arrows. **E:** Response to discrete field pulses perpendicular to the animal (90° and 270 °).3 seconds pulses of 2=V/cm were intermitted by 7 second lag phases of V=0. Field orientation is indicated by arrows **F:** Calcium transient in response to fields gradually rotating around the larval long axis, starting at 270 degrees. N=4 animals. Green: ΔF/F, light green= 1 SEM G: Scaling of neural response to field amplitude. An electric field of constant orientation of (180° in respect to the larva) was ramped from 0 to 2.5V/cm. N=4 animals. Green: ΔF/F, light green= 1 SEM

4.4.4 Molecular basis of electrotaxis

Nothing was known so far about the molecular components needed for detecting an electric field in invertebrates. We therefore aimed for identifying a receptor protein involved in electrotaxis, testing several mutant lines for the drosophila receptors which seemed to be plausible candidates for sensing electrical fields. We tested mutants devoid of cryptochrome, a receptor known to respond to magnetic fields (Yoshii, Ahmad et al. 2009) and a mutant for olfactory co-receptor Orco, since it is expressed in the DO sensory neurons. Both showed no impairment in the electrotaxis mass assay (Figure 4.4). Finally, we tested various mutants for members of the transient receptor potential (trp) family, which is known to be involved in a large range of sensory modalities (Damann,

Voets et al. 2008). We found that larvae devoid of functional receptors of the trp-C subclass, namely trp and trpl, respectively, were significantly impaired in electrotaxis performance, while none of the other receptors of the trp-family tested (trpA1, nanchung) had any effect. The fact that both trp and trpl mutants caused a defect fits with reports that they form heteromultimers and are partially redundant in function (Xu, Chien et al. 2000). For a more detailed analysis of the phenotype, we therefore used the $trp^{-/-}$, $trpl^{-/-}$ double mutant. Testing the double mutant in the high-resolution single animal assay we found that approach to the cathode was reduced and alignment to the field was less precise (Figure 4.4 B). Head casting was induced by the field switch, although less reliably and the alignment to the new field direction was slow and less accurate. Moreover, the animals overshot 90 degrees mean absolute bearing angle before inducing a turn during constant field conditions, which was never observed for wild type. Taken together, the phenotype was very similar to the one observed for NP2729>UAS-TNE, suggesting a role of the trp, trpl complex in the function of NP2729 labeled neurons.

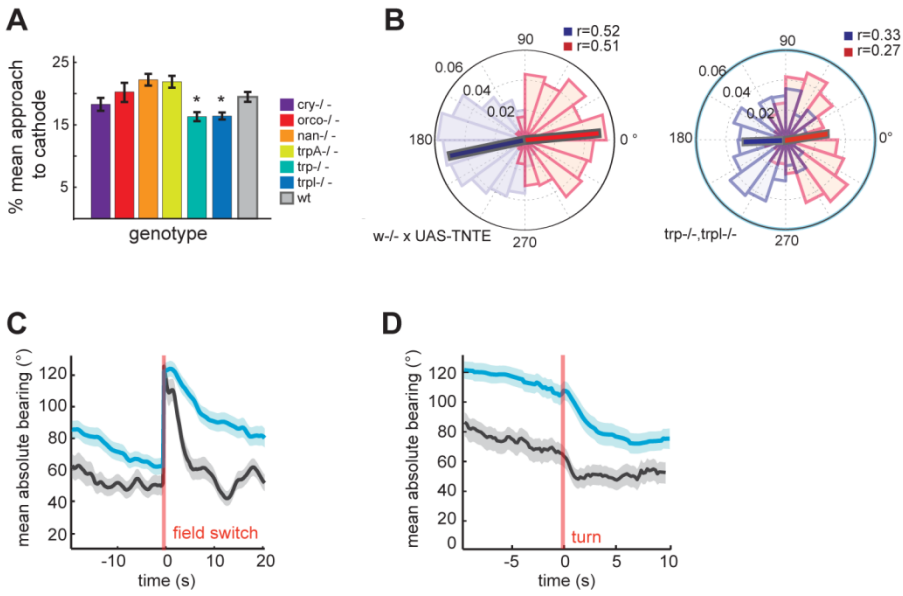

Figure 4.4 Trp and Trpl are involved in larval electrotaxis behavior. A: Binned mean approach to the cathode in an electrotaxis mass assay for various receptor mutants after 120 seconds of field exposure. * $p<0.05$ upon Bonferroni correction **B:** Polar plot of heading angles and circular mean for wild type (left panel) and trp, trpl- /- double mutant in a single animals assay. Blue and red indicate the respective field direction. Length of mean bars indicates circular variance (r). N=19 animals. **C:** Mean absolute bearing and after a field switch. N=18+-1animals. Shaded areas indicate 1SEM. **D:** Mean absolute bearing history prior and after turns during constant field conditions. N=18+-1animals, wt: 151 turns, trp,trpl-/-: 111 turns. Shaded areas indicate 1SEM, wt

4.5 Discussion

Despite of their small size and the reduced behavioral spectrum, D. *melanogaster* larvae use a multitude of sensory modalities to interact with their environment. Our study revealed yet another environmental cue which is detected: static electric fields. Although electric fields are ubiquitous and known to be used for orientation and prey or mate detection in several species, it was unknown until now if the widely used model organism *D. melanogaster* responds to electric fields. Our results

show that larvae robustly detect and navigate in electric fields ranging from 0.1 to 6 V/cm. Interestingly, the order of magnitude of the field strength is in agreement with those reported for other invertebrates, such as 3-14 V/cm for C. *elegans* or 10 V/cm for cockroach (Gabel, Gabel et al. 2007, Newland, Hunt et al. 2008). To navigate in the field, the larva must detect the direction of the field and coordinate its behavior aligning itself to a favorable direction in respect to the field. High-resolution analysis of single animal behavior revealed that larvae accurately orient towards the cathode when foraging in a uniform one-dimensional field. The underlying navigational strategy consists of keeping the run's bearing angle within a range of +/- 90 degrees to the field direction, resulting in a mean bearing of 45 degrees. Cast/turn episodes are induced when the bearing gets larger, being on average 80 prior to a turn, which improves alignment to the field after the turn. Accordingly, changes of field direction imposed on the animal are immediately detected; the animals use a cast/turn episode to align with the new polarity.

In a behavioral screen covering more than 1000 Gal4 enhancer trap lines, we identified neurons located in the terminal organ of the larvae which are involved in detection of the electric field. Silencing the respective neurons strongly reduces the fidelity of field detection. Using calcium imaging to report the neural activity in response to static electric fields, we could reveal the sensory encoding of field properties. Generally, the neural response increased with field strength. Stronger fields also led to more precise behavioral response, improving alignment to the field, probably reflecting the stronger response of the neurons to higher voltages. Secondly, the neurons were strongly activated when the animal was pointing towards the cathode and inhibited by opposed fields,

thus encoding direction of the field. Notably, this kind of neural bidirectional representation was found previously in other sensory modalities and species. A subset of larval odorant receptors respond with excitation or inhibition to different odors (Kreher, Kwon et al. 2005). In *C. elegans* chemotaxis in NaCl gradients, the ASE sensory neuron similarly engages in 2 different modes: it is inhibited upon rising and activated upon decreasing Cl^- concentrations (Suzuki, Thiele et al. 2008). Our results suggest that larvae orient towards the cathode in an attempt to avoid activation of these sensory neurons. Inhibition by positive fields may actively contribute to the approach behavior, e.g. by de-suppressing downstream neurons. Interestingly, tuning of sensory neurons to field direction was found also for *C elegans* and for single frog and guinea pig muscle cells (Tung, Sliz et al. 1991, Gabel, Gabel et al. 2007). In both cases, the strongest response was elicited by fields aligned to the long axis of the cell: C elegans neural activity peaked at 0° while myocyte contraction could be observed at 7 time lower voltages, when aligned to the field. Again threshold voltages (2.4+-0.6 V/cm) were similar to the field strengths sensed by *Drosophila* larvae.

What may be the mechanism underlying neural response to electric field? Since we found a specific type of neurons responding to the field, we conclude that the response is not a general property of neurons being polarized by the applied field. Moreover, the implication of the trp-c receptor subfamily hints to a detection of the field via a receptor being sensitive to field changes and polarity. Yet, responses of muscle tissue to the field could contribute to the taxis behavior observed. In fact we could observe contraction of muscles due to the applied field during imaging. This contribution could explain the incomplete nature of the loss of

function phenotype when silencing sensory neurons as well as in trp mutants. Both manipulations strongly reduce fidelity of orientation and approach towards the cathode, although never completely abolishing it. Trp and trpl are also implicated in other sensory modalities of *Drosophila melanogaster*: cold sensing and photodetection (Rosenzweig, Kang et al. 2008), being the major route for cation entry into the drosophila photoreceptor cell after photon absorption. It was recently proposed that the light induced cascade activates Phospholipase C, which cleaves membrane phospholipid PIP_2 into smaller molecules causes changes of the physical properties and acidification of the photoreceptor cell membrane. The resulting mechanical forces cause the activation of trp and trpl channels (Hardie and Franze 2012). A similar mechanism was proposed for mouse temperature sensitive trps (Clapham 2003). Recently however, Voets et al. came to a different conclusion when investigating the principles of temperature sensing by mouse trp channels (Voets, Droogmans et al. 2004). They found that the channels are voltage gated and temperature changes activate TrpM8 by a shift of the voltage dependence of its activation. This mechanism is membrane autonomous, meaning that - in contrast to *Drosophila* - no second messengers are to gate the channel, but opening is caused solely through thermodynamical changes in channel structure. It is also known that cell membranes reorganize upon exposure to static fields causing cell polarization and migration (McCaig, Rajnicek et al. 2005). Hence, we speculate that either changes of membrane state and composition or the conformation of the channel itself may be changed by the field forces, causing calcium influx and action potentials. It also seems plausible that the electric field minimally deforms the neurons and resulting mechanical forces cause the

channels to open. The role of the trp receptors could be further tested by probing neural activity in a trp or trpl mutant or using a trp inhibitor. It would be desirable to allocate expression of the trp channels to the electrosensory neurons e.g. by immunolabelling. Another factor which we cannot rule out to contribute is a magnetic field. Given the static nature of the electric field, the electrotaxis arena cannot be the source of magnetism. However, the larva itself can be interpreted as ions moving in an electric field, therefore causing a magnetic field. In fact, it was shown recently that larvae respond to magnetic fields, choosing a preferred heading orientation depending on field orientation during development (Dommer, Gazzolo et al. 2008). For investigating a possible contribution of electromagnetic phenomena to the neural activity in responses to magnetic fields should be tested.

In contrast to extraordinary robustness of electrotaxis and its prevalence in various invertebrate species, the ecological relevance of this sense remains unknown. We speculate that the direction of electric fields may be informative for the larvae in their natural habitat, such as rotting fruits. It would be highly interesting to know about the electric properties of whole fruits or within its subcompartments, e.g. a voltage potential between the pulp and the peel or at peel fissures. Maybe because of the lack of a human electric sensory modality, electric fields are a frequently neglected dimension of sensory perception. The frequent occurrence in other species, however, suggests electric field sensing as a potentially important sensory modality, which now should be considered alongside vision and olfaction. Our results represent a basis for further investigation of the electric senses and their role for invertebrate and vertebrate behavior.

Chapter 5

General discussion and further directions

Understanding how nervous systems create behavior is the fundamental challenge in neuroscience. After all it is a common notion that it is the brain's capacity that sets humans apart from other species. However, our advance towards understanding a brain at the level of its single neurons is hampered by its outstanding complexity in higher phyla such as vertebrates or mammals. Therefore invertebrate model organisms harboring nervous systems of a few hundred to several thousand neurons represent an eligible tradeoff between complexity and traceability. This notion led to a surge of neurobiological studies in species like *Drosophila melanogaster, Acrididae* (locust) and *Caenorhabditis* elegans in the last decades. Among invertebrate models, *Drosophila* has several significant advantages: It harbors a central nervous system, just like vertebrates. The long history of *Drosophila* research has led to a multitude of well-established techniques, which let us tackle problems from various perspectives, ranging from the molecular level of the function of single proteins to the macroscopic level like behavioral output (Venken, Simpson et al. 2011). Additionally, the fruit fly exhibits a wide range of behaviors which cover the repertoire of basic animal actions such as food- and mate-search, courtship and social behaviors like aggression and learning and memory retrieval. Accordingly, it can be used as a model for complex human neurodegenerative diseases like Parkinson, Alzheimer

and attention-deficit hyperactivity disorder (Bilen and Bonini 2005, van Swinderen and Brembs 2010).

In an attempt to further reduce the number of neurons while still exploiting the organisms experimental potential, we decided to investigate the *Drosophila* larva. Strikingly, the larval brain conserves major anatomical and functional features of the adult and even mammals, being 100 times smaller than the adult in number (Gerber and Stocker 2007). The aim of this study was to identify novel neural populations underlying larval behavioral organization connecting known primary sensory input to behavioral output. In a screen we targeted tetanus toxin to genetically defined subpopulations of the larval brain and quantified the effects of our manipulation on chemo- and electrotaxis behavior. We could identify a group of neurons in the suboesophageal ganglion (SOG) to be involved in initiation and execution of cast/turn events, which serves to orient the animal towards sensory cues. Remarkably, activation of this neurons was sufficient to elicit a cast/turn maneuver. Our study therefore identified for the first time neurons involved in larval locomotion initiation, controlling the switch from run to cast/turn mode.

The SOG demarks the neuropil connection between the brain lobes and the VNC. It is a well documented entry site for gustatory sensory information. Detection of chemical compunds like sugar or NaCl cause attraction or avoidance repsectively, therefore modifying navigational decisions (Schwartz, Zhong et al. 2012). Yet, it is not only a taste integration center as several studies are linking it to a range of behavioral modalities. First, other sensory modalities convey primary information to the SOG: thermosensation and electrosensation. Luo et al showed that

thermotaxis relies on run length modulation based on thermosensory input to the SOG (Luo, Gershow et al. 2010). The present study shows that also electrosensory neurons project to the SOG. Activaton of these neurons causes headcasting/turn events, therefore interrupting run phases. It would be intriguing to elucidate if the run modulation and/or cast initiation Other Gal4 lines covering specificly neurons in the SOG and intersectional tools supressing activity in other brain regions would be useful to further investigate these questions. Techniques which report connectivity or close vicinity of two neural populations (photoactivatable GFP, GRASP), could reveal existing secondary interneurons receiving input from one or various sensory modalitys which feed to the SOG (Feinberg, Vanhoven et al. 2008, Lai, Lo et al. 2012).

Secondly, several types of biogenic amine secreting neurons and neurons with their respective receptor reside or arborize in the SOG (Selcho, Pauls et al. 2009). These include dopamine, serotonine and octopamine. Biogenic amines are well known for their role as modifiers of behavior. Zhou et al showed that a subset of octopaminergic neurons located in the adult *Drosophila* SOG is important for aggression (Zhou, Rao et al. 2008). Selcho et al proposed dopaminergic neurons innervating the SOG may control naive gustatory responses (Selcho, Pauls et al. 2009). At the same time, most recently the execution of basic locomotor function such as forward crawling and turning could be attributed exclusively to the VNC, showing that the SOG is not underlying the mere execution of behavioral patterns (Berni, Pulver et al. 2012, Selcho, Pauls et al. 2012).

Based on these previous findings and our own results we conclude that the SOG may represent an area of behavioral modulation comprehensive for several sensory modalities. We speculate that this part of the brain neuropil functionally connects the lobes (essential for primary sensory integration of vision and olfaction) to the VNC (locomotor output) controlling selection and execution of behavioral modes.

Further studies using optogenetics for controlling and calcium imaging for monitoring neural activity should reveal the function of these cells in more detail. It would be desirable to elucidate the nature of the neural activity of the identified neurons underlying their modifying role. Moreover it would be highly interesting to clarify the connectivity of the pre- and postsynaptic partners in the SOG. An attempt for establishing such a connectome based on electron microscopy data of the first instar larval brain is currently undertaken (Cardona, Saalfeld et al. 2010), hence we assume it will be possible to establish a wiring diagram similar to the one for *C. elegans* in the near future, informing about connectivity at the level of individual neuronal processes and synapse also in the SOG.

In a second part of our study we focused on the behavior of *Drosophila* larvae in response to static electric fields and their sensory system underlying it. We found that larvae robustly navigate to the cathode. Orientation responses to electric fields was reported for a growing number of species, in particular several invertebrate studies were published in the last years (Gabel, Gabel et al. 2007, Newland, Hunt et al. 2008, Shapiro-Ilan, Lewis et al. 2012, Clarke, Whitney et al. 2013, Greggers, Koch et al. 2013). Stunningly, in the vast majority occurrences of electrotaxis-ranging from single cell migration to invertebrate organism

behavioral response- the direction of movement is towards the cathode. The reason and the biological relevance of this phenomenon remain to be revealed. In accordance with findings for *C. elegans* larval sensory neurons are excited when aligned to electric field lines and inhibited when pointing in the converse direction. The behavioral response can be interpreted as avoidance of the electrosensory activity, therefore causing migration towards the cathode. Despite of the robust response, the ethological relevance of this behavior remains unclear. One can speculate that electric fields occurring in the natural habitat of *Drosophila* larvae are used for orientation. In fact plants have an electric potential along their stem and appendices, which was shown to be detected by bees (Gurovich and Hermosilla 2009, Clarke, Whitney et al. 2013). Equally local fields in a rotting fruit could be a cue for the larva, e.g. signaling noxious conditions to be avoided.

Taken together the present study gives new insight in types of sensory stimuli detected and how this sensory information is converted into specific behavioral output. I humbly hope that it can add to our understanding of neural systems and maybe contributes to further investigation on how behaviors are elicited and controlled.

References

Adler, J. and W. Shi (1988). "Galvanotaxis in bacteria." Cold Spring Harb Symp Quant Biol **53 Pt 1**: 23-25.

Akerboom, J., J. D. Rivera, M. M. Guilbe, E. C. Malave, H. H. Hernandez, L. Tian, S. A. Hires, J. S. Marvin, L. L. Looger and E. R. Schreiter (2009). "Crystal structures of the GCaMP calcium sensor reveal the mechanism of fluorescence signal change and aid rational design." J Biol Chem **284**(10): 6455-6464.

Asahina, K., M. Louis, S. Piccinotti and L. B. Vosshall (2009). "A circuit supporting concentration-invariant odor perception in Drosophila." J Biol **8**(1): 9.

Baier, A., B. Wittek and B. Brembs (2002). "Drosophila as a new model organism for the neurobiology of aggression?" J Exp Biol **205**(Pt 9): 1233-1240.

Bednar, J., P. Furrer, V. Katritch, A. Z. Stasiak, J. Dubochet and A. Stasiak (1995). "Determination of DNA persistence length by cryo-electron microscopy. Separation of the static and dynamic contributions to the apparent persistence length of DNA." J Mol Biol **254**(4): 579-594.

Benzer, S. (1967). "BEHAVIORAL MUTANTS OF Drosophila ISOLATED BY COUNTERCURRENT DISTRIBUTION." Proc Natl Acad Sci U S A **58**(3): 1112-1119.

Berni, J., S. R. Pulver, L. C. Griffith and M. Bate (2012). "Autonomous circuitry for substrate exploration in freely moving Drosophila larvae." Curr Biol **22**(20): 1861-1870.

Bilen, J. and N. M. Bonini (2005). "Drosophila as a model for human neurodegenerative disease." Annu Rev Genet **39**: 153-171.

Cardona, A., S. Saalfeld, S. Preibisch, B. Schmid, A. Cheng, J. Pulokas, P. Tomancak and V. Hartenstein (2010). "An integrated micro- and macroarchitectural analysis of the Drosophila brain by computer-assisted serial section electron microscopy." PLoS Biol **8**(10).

Cardona, A., S. Saalfeld, P. Tomancak and V. Hartenstein (2009). "Drosophila brain development: closing the gap between a macroarchitectural and microarchitectural approach." Cold Spring Harb Symp Quant Biol **74**: 235-248.

Chou, Y. H., M. L. Spletter, E. Yaksi, J. C. Leong, R. I. Wilson and L. Luo (2010). "Diversity and wiring variability of olfactory local interneurons in the Drosophila antennal lobe." Nat Neurosci **13**(4): 439-449.

Clapham, D. E. (2003). "TRP channels as cellular sensors." Nature **426**(6966): 517-524.

Clarke, D., H. Whitney, G. Sutton and D. Robert (2013). "Detection and Learning of Floral Electric Fields by Bumblebees." Science.

Clyne, J. D. and G. Miesenbock (2008). "Sex-specific control and tuning of the pattern generator for courtship song in Drosophila." Cell **133**(2): 354-363.

Colomb, J., N. Grillenzoni, A. Ramaekers and R. F. Stocker (2007). "Architecture of the primary taste center of Drosophila melanogaster larvae." J Comp Neurol **502**(5): 834-847.

Damann, N., T. Voets and B. Nilius (2008). "TRPs in our senses." Curr Biol **18**(18): R880-889.

Das, A., T. Gupta, S. Davla, L. L. Prieto-Godino, S. Diegelmann, O. V. Reddy, K. V. Raghavan, H. Reichert, J. Lovick and V. Hartenstein (2013). "Neuroblast lineage-specific origin of the neurons of the Drosophila larval olfactory system." Dev Biol **373**(2): 322-337.

Dommer, D. H., P. J. Gazzolo, M. S. Painter and J. B. Phillips (2008). "Magnetic compass orientation by larval Drosophila melanogaster." J Insect Physiol **54**(4): 719-726.

Feinberg, E. H., M. K. Vanhoven, A. Bendesky, G. Wang, R. D. Fetter, K. Shen and C. I. Bargmann (2008). "GFP Reconstitution Across Synaptic Partners (GRASP) defines cell contacts and synapses in living nervous systems." Neuron **57**(3): 353-363.

Fox, L. E., D. R. Soll and C. F. Wu (2006). "Coordination and modulation of locomotion pattern generators in Drosophila larvae: effects of altered biogenic amine levels by the tyramine beta hydroxlyase mutation." J Neurosci **26**(5): 1486-1498.

Friesen, W. O. and W. B. Kristan (2007). "Leech locomotion: swimming, crawling, and decisions." Curr Opin Neurobiol **17**(6): 704-711.

Gabel, C. V., H. Gabel, D. Pavlichin, A. Kao, D. A. Clark and A. D. Samuel (2007). "Neural circuits mediate electrosensory behavior in Caenorhabditis elegans." J Neurosci **27**(28): 7586-7596.

Galvani, L. (1791). " De Viribus Electricitatis in Motu Musculari Commentarius." Ex typographia Instituti Scientiarum.

Garrity, P. A., M. B. Goodman, A. D. Samuel and P. Sengupta (2010). "Running hot and cold: behavioral strategies, neural circuits, and the molecular machinery for thermotaxis in C. elegans and Drosophila." Genes Dev **24**(21): 2365-2382.

Gerber, B. and R. F. Stocker (2007). "The Drosophila larva as a model for studying chemosensation and chemosensory learning: a review." Chem Senses **32**(1): 65-89.

Gill, D. M. (1982). "Bacterial toxins: a table of lethal amounts." Microbiol Rev **46**(1): 86-94.

Gomez-Marin, A. and M. Louis (2012). "Active sensation during orientation behavior in the Drosophila larva: more sense than luck." Curr Opin Neurobiol **22**(2): 208-215.

Gomez-Marin, A., N. Partoune, G. J. Stephens and M. Louis (2012). "Automated Tracking of Animal Posture and Movement during Exploration and Sensory Orientation Behaviors." PLoS One **7**(8): e41642.

Gomez-Marin, A., G. J. Stephens and M. Louis (2011). "Active sampling and decision making in Drosophila chemotaxis." Nat Commun **2**: 441.

Gong, Z., J. Liu, C. Guo, Y. Zhou, Y. Teng and L. Liu (2010). "Two pairs of neurons in the central brain control Drosophila innate light preference." Science **330**(6003): 499-502.

Gordon, M. D. and K. Scott (2009). "Motor control in a Drosophila taste circuit." Neuron **61**(3): 373-384.

Gow, N. A. (1994). "Growth and guidance of the fungal hypha." Microbiology **140 (Pt 12)**: 3193-3205.

Green, C. H., B. Burnet and K. J. Connolly (1983). "Organization and patterns of inter- and intraspecific variation in the behaviour of Drosophila larvae." Animal Behaviour **31**(1): 282-291.

Greggers, U., G. Koch, V. Schmidt, A. Durr, A. Floriou-Servou, D. Piepenbrock, M. C. Gopfert and R. Menzel (2013). "Reception and learning of electric fields in bees." Proc Biol Sci **280**(1759): 20130528.

Grueber, W. B., L. Y. Jan and Y. N. Jan (2002). "Tiling of the Drosophila epidermis by multidendritic sensory neurons." Development **129**(12): 2867-2878.

Gurovich, L. A. and P. Hermosilla (2009). "Electric signalling in fruit trees in response to water applications and light-darkness conditions." J Plant Physiol **166**(3): 290-300.

Hallem, E. A. and J. R. Carlson (2006). "Coding of odors by a receptor repertoire." Cell **125**(1): 143-160.

Hamada, F. N., M. Rosenzweig, K. Kang, S. R. Pulver, A. Ghezzi, T. J. Jegla and P. A. Garrity (2008). "An internal thermal sensor controlling temperature preference in Drosophila." Nature **454**(7201): 217-220.

Hardie, R. C. and K. Franze (2012). "Photomechanical responses in Drosophila photoreceptors." Science **338**(6104): 260-263.

Hayashi, S., K. Ito, Y. Sado, M. Taniguchi, A. Akimoto, H. Takeuchi, T. Aigaki, F. Matsuzaki, H. Nakagoshi, T. Tanimura, R. Ueda, T. Uemura, M. Yoshihara and S. Goto (2002). "GETDB, a database

compiling expression patterns and molecular locations of a collection of Gal4 enhancer traps." Genesis **34**(1-2): 58-61.

Herculano-Houzel, S. (2009). "The human brain in numbers: a linearly scaled-up primate brain." Front Hum Neurosci **3**: 31.

Hires, S. A., L. Tian and L. L. Looger (2008). "Reporting neural activity with genetically encoded calcium indicators." Brain Cell Biol **36**(1-4): 69-86.

Hotta, Y. and S. Benzer (1970). "Genetic dissection of the Drosophila nervous system by means of mosaics." Proc Natl Acad Sci U S A **67**(3): 1156-1163.

Ingvar, S. (1920). "Reaction of cells to the galvanic current in tissue cultures." Experimental Biology and Medicine **17**(8): 198-199.

Keene, A. C. and S. G. Sprecher (2012). "Seeing the light: photobehavior in fruit fly larvae." Trends Neurosci **35**(2): 104-110.

Kitamoto, T. (2002). "Conditional disruption of synaptic transmission induces male-male courtship behavior in Drosophila." Proc Natl Acad Sci U S A **99**(20): 13232-13237.

Koch, C. and G. Laurent (1999). "Complexity and the nervous system." Science **284**(5411): 96-98.

Kohsaka, H., S. Okusawa, Y. Itakura, A. Fushiki and A. Nose (2012). "Development of larval motor circuits in Drosophila." Dev Growth Differ **54**(3): 408-419.

Korohoda, W., M. Mycielska, E. Janda and Z. Madeja (2000). "Immediate and long-term galvanotactic responses of Amoeba proteus to dc electric fields." Cell Motil Cytoskeleton **45**(1): 10-26.

Kreher, S. A., J. Y. Kwon and J. R. Carlson (2005). "The molecular basis of odor coding in the Drosophila larva." Neuron **46**(3): 445-456.

Lahiri, S., K. Shen, M. Klein, A. Tang, E. Kane, M. Gershow, P. Garrity and A. D. Samuel (2011). "Two alternating motor programs drive navigation in Drosophila larva." PLoS One **6**(8): e23180.

Lai, J. S., S. J. Lo, B. J. Dickson and A. S. Chiang (2012). "Auditory circuit in the Drosophila brain." Proc Natl Acad Sci U S A **109**(7): 2607-2612.

Lai, S. L. and T. Lee (2006). "Genetic mosaic with dual binary transcriptional systems in Drosophila." Nat Neurosci **9**(5): 703-709.

Larsson, M. C., A. I. Domingos, W. D. Jones, M. E. Chiappe, H. Amrein and L. B. Vosshall (2004). "Or83b encodes a broadly expressed odorant receptor essential for Drosophila olfaction." Neuron **43**(5): 703-714.

Leinwand, S. G. and S. H. Chalasani (2011). "Olfactory networks: from sensation to perception." Curr Opin Genet Dev **21**(6): 806-811.

Louis, M., T. Huber, R. Benton, T. P. Sakmar and L. B. Vosshall (2008). "Bilateral olfactory sensory input enhances chemotaxis behavior." Nat Neurosci **11**(2): 187-199.

Luo, L., M. Gershow, M. Rosenzweig, K. Kang, C. Fang-Yen, P. A. Garrity and A. D. Samuel (2010). "Navigational decision making in Drosophila thermotaxis." J Neurosci **30**(12): 4261-4272.

Marella, S., K. Mann and K. Scott (2012). "Dopaminergic modulation of sucrose acceptance behavior in Drosophila." Neuron **73**(5): 941-950.

McCaig, C. D., A. M. Rajnicek, B. Song and M. Zhao (2005). "Controlling cell behavior electrically: current views and future potential." Physiol Rev **85**(3): 943-978.

McCaig, C. D., B. Song and A. M. Rajnicek (2009). "Electrical dimensions in cell science." J Cell Sci **122**(Pt 23): 4267-4276.

McGuire, S. E., Z. Mao and R. L. Davis (2004). "Spatiotemporal gene expression targeting with the TARGET and gene-switch systems in Drosophila." Sci STKE **2004**(220): pl6.

Newland, P. L., E. Hunt, S. M. Sharkh, N. Hama, M. Takahata and C. W. Jackson (2008). "Static electric field detection and behavioural avoidance in cockroaches." J Exp Biol **211**(Pt 23): 3682-3690.

Nusslein-Volhard, C. and E. Wieschaus (1980). "Mutations affecting segment number and polarity in Drosophila." Nature **287**(5785): 795-801.

Pauls, D., M. Selcho, N. Gendre, R. F. Stocker and A. S. Thum (2010). "Drosophila larvae establish appetitive olfactory memories via mushroom body neurons of embryonic origin." J Neurosci **30**(32): 10655-10666.

Pierce-Shimomura, J. T., T. M. Morse and S. R. Lockery (1999). "The fundamental role of pirouettes in Caenorhabditis elegans chemotaxis." J Neurosci **19**(21): 9557-9569.

Potter, C. J., B. Tasic, E. V. Russler, L. Liang and L. Luo (2010). "The Q system: a repressible binary system for transgene expression, lineage tracing, and mosaic analysis." Cell **141**(3): 536-548.

Pulver, S. R., S. L. Pashkovski, N. J. Hornstein, P. A. Garrity and L. C. Griffith (2009). "Temporal dynamics of neuronal activation by Channelrhodopsin-2 and TRPA1 determine behavioral output in Drosophila larvae." J Neurophysiol **101**(6): 3075-3088.

Rajan, R., J. P. Clement and U. S. Bhalla (2006). "Rats smell in stereo." Science **311**(5761): 666-670.

Robinson, K. R. (1985). "The responses of cells to electrical fields: a review." J Cell Biol **101**(6): 2023-2027.

Rosenzweig, M., K. Kang and P. A. Garrity (2008). "Distinct TRP channels are required for warm and cool avoidance in Drosophila melanogaster." Proc Natl Acad Sci U S A **105**(38): 14668-14673.

Sato, M. J., M. Ueda, H. Takagi, T. M. Watanabe, T. Yanagida and M. Ueda (2007). "Input-output relationship in galvanotactic response of Dictyostelium cells." Biosystems **88**(3): 261-272.

Schwartz, N. U., L. Zhong, A. Bellemer and W. D. Tracey (2012). "Egg laying decisions in Drosophila are consistent with foraging costs of larval progeny." PLoS One **7**(5): e37910.

Selcho, M., D. Pauls, B. El Jundi, R. F. Stocker and A. S. Thum (2012). "The role of octopamine and tyramine in Drosophila larval locomotion." J Comp Neurol **520**(16): 3764-3785.

Selcho, M., D. Pauls, K. A. Han, R. F. Stocker and A. S. Thum (2009). "The role of dopamine in Drosophila larval classical olfactory conditioning." PLoS One **4**(6): e5897.

Shapiro-Ilan, D. I., E. E. Lewis, J. F. Campbell and D. B. Kim-Shapiro (2012). "Directional movement of entomopathogenic nematodes in response to electrical field: effects of species, magnitude of voltage, and infective juvenile age." J Invertebr Pathol **109**(1): 34-40.

Shimizu, T. S., Y. Tu and H. C. Berg (2010). "A modular gradient-sensing network for chemotaxis in Escherichia coli revealed by responses to time-varying stimuli." Mol Syst Biol **6**: 382.

Siingh D, S. A. K. (2006). "The atmospheric global electric circuit: An overview." Atmospheric Research **84**: 91-110.

Sprecher, S. G., A. Cardona and V. Hartenstein (2011). "The Drosophila larval visual system: high-resolution analysis of a simple visual neuropil." Dev Biol **358**(1): 33-43.

Stockinger, P., D. Kvitsiani, S. Rotkopf, L. Tirian and B. J. Dickson (2005). "Neural circuitry that governs Drosophila male courtship behavior." Cell **121**(5): 795-807.

Suzuki, H., T. R. Thiele, S. Faumont, M. Ezcurra, S. R. Lockery and W. R. Schafer (2008). "Functional asymmetry in Caenorhabditis elegans taste neurons and its computational role in chemotaxis." Nature **454**(7200): 114-117.

Sweeney, S. T., K. Broadie, J. Keane, H. Niemann and C. J. O'Kane (1995). "Targeted expression of tetanus toxin light chain in Drosophila specifically eliminates synaptic transmission and causes behavioral defects." Neuron **14**(2): 341-351.

Thesen, A., J. B. Steen and K. B. Doving (1993). "Behaviour of dogs during olfactory tracking." J Exp Biol **180**: 247-251.

Thum, A. S., S. Knapek, J. Rister, E. Dierichs-Schmitt, M. Heisenberg and H. Tanimoto (2006). "Differential potencies of effector genes in adult Drosophila." J Comp Neurol **498**(2): 194-203.

Thum, A. S., B. Leisibach, N. Gendre, M. Selcho and R. F. Stocker (2011). "Diversity, variability, and suboesophageal connectivity of antennal lobe neurons in D. melanogaster larvae." J Comp Neurol **519**(17): 3415-3432.

Tian, L., S. A. Hires, T. Mao, D. Huber, M. E. Chiappe, S. H. Chalasani, L. Petreanu, J. Akerboom, S. A. McKinney, E. R. Schreiter, C. I. Bargmann, V. Jayaraman, K. Svoboda and L. L. Looger (2009). "Imaging neural activity in worms, flies and mice with improved GCaMP calcium indicators." Nat Methods **6**(12): 875-881.

Truman, J. W. and L. M. Riddiford (1999). "The origins of insect metamorphosis." Nature **401**(6752): 447-452.

Tung, L., N. Sliz and M. R. Mulligan (1991). "Influence of electrical axis of stimulation on excitation of cardiac muscle cells." Circ Res **69**(3): 722-730.

Tunstall, N. E., A. Herr, M. de Bruyne and C. G. Warr (2012). "A screen for genes expressed in the olfactory organs of Drosophila melanogaster identifies genes involved in olfactory behaviour." PLoS One **7**(4): e35641.

Usha, N. and L. S. Shashidhara (2010). "Interaction between Ataxin-2 Binding Protein 1 and Cubitus-interruptus during wing development in Drosophila." Dev Biol **341**(2): 389-399.

van Swinderen, B. and B. Brembs (2010). "Attention-like deficit and hyperactivity in a Drosophila memory mutant." J Neurosci **30**(3): 1003-1014.

Venken, K. J., J. H. Simpson and H. J. Bellen (2011). "Genetic manipulation of genes and cells in the nervous system of the fruit fly." Neuron **72**(2): 202-230.

Voets, T., G. Droogmans, U. Wissenbach, A. Janssens, V. Flockerzi and B. Nilius (2004). "The principle of temperature-dependent gating in

cold- and heat-sensitive TRP channels." Nature **430**(7001): 748-754.

Wang, J. W., A. M. Wong, J. Flores, L. B. Vosshall and R. Axel (2003). "Two-photon calcium imaging reveals an odor-evoked map of activity in the fly brain." Cell **112**(2): 271-282.

Wang, Y., Y. Pu and P. Shen (2013). "Neuropeptide-Gated Perception of Appetitive Olfactory Inputs in Drosophila Larvae." Cell Rep.

Wilson, R. I., G. C. Turner and G. Laurent (2004). "Transformation of olfactory representations in the Drosophila antennal lobe." Science **303**(5656): 366-370.

Wueringer, B. E. (2012). "Electroreception in elasmobranchs: sawfish as a case study." Brain Behav Evol **80**(2): 97-107.

Xiang, Y., Q. Yuan, N. Vogt, L. L. Looger, L. Y. Jan and Y. N. Jan (2010). "Light-avoidance-mediating photoreceptors tile the Drosophila larval body wall." Nature **468**(7326): 921-926.

Xu, X. Z., F. Chien, A. Butler, L. Salkoff and C. Montell (2000). "TRPgamma, a drosophila TRP-related subunit, forms a regulated cation channel with TRPL." Neuron **26**(3): 647-657.

Yao, Z., A. M. Macara, K. R. Lelito, T. Y. Minosyan and O. T. Shafer (2012). "Analysis of functional neuronal connectivity in the Drosophila brain." J Neurophysiol **108**(2): 684-696.

Yoshii, T., M. Ahmad and C. Helfrich-Forster (2009). "Cryptochrome mediates light-dependent magnetosensitivity of Drosophila's circadian clock." PLoS Biol **7**(4): e1000086.

Zhou, C., Y. Rao and Y. Rao (2008). "A subset of octopaminergic neurons are important for Drosophila aggression." Nat Neurosci **11**(9): 1059-1067.